Anna Popova

ORCID 0000-0002-3916-4040

The Role of B-Cell Differentiation and Gut Microbiome in the Pathogenesis and Progression of IgA Nephropathy

Summary of the Doctoral Thesis for obtaining the scientific degree "Doctor of Science (*PhD*)"

Sector Group – Medical and Health Sciences

Sector – Clinical Medicine

Sub-Sector – Internal Medicine

Riga, 2026

The Doctoral Thesis was developed at Rīga Stradiņš University, Pauls Stradins Clinical University Hospital, Latvia

Supervisors of the Doctoral Thesis:

Dr. med., Associate Professor **Viktorija Kuzema**,
Rīga Stradiņš University, Department of Internal Diseases, Latvia

Dr. med., Professor **Juta Kroiča**,
Rīga Stradiņš University, Department of Biology and Microbiology, Latvia

Official Reviewers:

Dr. med., Professor **Nataļja Kurjāne**,
Rīga Stradiņš University, Department of Biology and Microbiology, Latvia

Dr. med., **Jeļizaveta Sokolovska**,
University of Latvia, Faculty of Medicine and Life Sciences

Dr. med., Professor **Ivan Rychlik**,
Charles University, Department of Internal Medicine, Czech Republic

Defence of the Doctoral Thesis will take place at the public session of the Promotion Council of Clinical Medicine on 2 February 2026 at 11.00 in in the Boris Teterev Auditorium, 26A Anniņmuižas Boulevard, Rīga Stradiņš University Medical Education Technology Centre

The Doctoral Thesis is available in RSU Library and on RSU website:
https://www.rsu.lv/en/dissertations

Research project was supported by RSU *PhD* grant

Latvian Council of Science

Research project was supported by the Fundamental and Applied Research
Project No lzp-2019/1-0139 “Dissecting the interplay between intestinal dysbiosis and
B cell function in the pathogenesis of immunoglobulin A nephropathy”

Secretary of the Promotion Council:

PhD, Assistant **Dana Kigitoviča**

Table of Contents

Abbreviations used in the Thesis 4

Introduction 5
- Aim of the Thesis 6
- Tasks of the Thesis 6
- Hypotheses of the Thesis 6
- Novelty of the Thesis 7

1 Materials and Methods 8
- 1.1 Patient characteristics 8
- 1.2 Clinical laboratory tests 9
- 1.3 Analysis of the differentiation of IgA+ plasmablasts 9
- 1.4 Gut microbiome analysis 10
- 1.5 Statistical analysis 11

2 Results 13
- 2.1 Kidney survival and its associated clinical and histological risk factors 13
- 2.2 Prediction of kidney function decline by Cox regression and the International IgAN Prediction Tool 17
- 2.3 B cell activation pathways in IgAN patients 18
- 2.4 Characteristics of gut microbiome composition in IgAN patients 22

3 Discussion 27

Conclusions 37

Proposals 38

List of publications, reports and patents on the topic of the Thesis 39

References 41

Acknowledgements 46

Abbreviations used in the Thesis

ACEI	angiotensin-converting enzyme inhibitors
ARB	angiotensin II receptor blockers
ASC	antibody-secreting cells
BMI	body mass index
C	crescents
CKD	chronic kidney disease
DBP	diastolic blood pressure
DN	double negative
DNA	deoxyribonucleic acid
E	endocapillary cellularity
EDTA	ethylenediaminetetraacetic acid
eGFR	estimated glomerular filtration rate
ESKD	end-stage kidney disease
FDR	false discovery rate
Gd-IgA1	galactose-deficient IgA1
HC	healthy controls
ICC	intraclass correlation coefficient
IgAN	immunoglobulin A nephropathy
IIgANPT	International IgAN Prediction Tool
LPS	lipopolysaccharides
M	mesangial hypercellularity
PBMC	peripheral blood mononuclear cell
PBS	phosphate-buffered solution
S	segmental sclerosis
SBP	systolic blood pressure
T	interstitial fibrosis / tubular atrophy
TLR	toll-like receptor
Tregs	regulatory T cells
UPCR	urine protein-to-creatinine ratio

Introduction

French pathologist named Dr. Jean Berger, along with his colleague Dr. Nicole Hinglais in 1968 initially defined immunoglobulin A nephropathy (IgAN) as a kidney disorder marked by glomerular "intercapillary deposits of IgA-IgG" (Berger & Hinglais, 1968). The renal biopsy typically reveals predominant IgA glomerular deposits performing immunofluorescence, often accompanied by mesangial cell proliferation and matrix expansion. IgAN is the most prevalent primary glomerular disease in numerous countries and continues to be a significant contributor to chronic kidney disease (CKD) and end-stage kidney disease (ESKD) (Rajasekaran et al., 2021). Geographical variation in distribution and the galactose-deficient IgA1 (Gd-IgA1) inheritance trait highlight the potential influence of both environment and genetics on susceptibility to IgAN (Du et al., 2023).

IgAN clinically presents in diverse manifestations: episodes of macrohaematuria, microscopic changes in urinalysis, nephritic syndrome, nephrotic syndrome and rapidly progressive glomerulonephritis. The clinical course can vary, but on average 30–40 % of patients reach terminal kidney failure within 20–30 years of diagnosis, and the disease may recur in the kidney graft (Lai et al., 2016). As the prognosis of this disease varies according to its manifestation, the International IgAN Prediction Tool (IIgANPT) was investigated in 2019. It integrates validated clinicopathological prognostic factors with treatments received at the time of diagnosis to generate an individualised risk of disease progression, supporting patient counselling, and facilitating shared decision-making (Barbour et al., 2019). The IIgANPT has undergone external validation across different ethnic groups, producing varying results. Until 2021, it had only been validated in non-European cohorts: Chinese-Argentinian (Zhang et al., 2020) and Korean (Hwang et al., 2021).

According to existing evidence, IgA nephropathy is believed to result from a combination of various pathogenic factors rather than a singular cause. The increased presence of circulating polymeric Gd-IgA1 and the generation of O-glycan-specific antibodies contribute to the development of immune complexes containing IgA1. The subsequent deposition of these complexes in the mesangium triggers inflammation and leads to glomerular damage (Yeo et al., 2018). B cells play a central role in the pathogenesis by serving as the origin of Gd-IgA1 and producing autoantibodies against it (Scionti et al., 2022). However, significant gaps exist in our understanding of the activation and differentiation pathways of B cells that result in the secretion of pathogenic IgA antibodies in IgAN. Individual reports have delineated specific aspects of B cell activation, including a decrease in regulatory B cells (Wang et al., 2014), reduced proportion of pre-switched B cells and plasmablasts, an increase in long-lived plasma cells in the peripheral circulation (Sendic et al.,

2021) and heightened expression of toll-like receptor 7 (TLR) in circulating B cells (Zheng et al., 2020). However, the exploration of B cell activation pathways remains unexplored and awaits incorporation into the overall understanding of the etiopathogenesis of IgAN.

Increasing evidence establishes a significant connection between the gut mucosal system and IgAN. In line with this, genome-wide association studies have pinpointed numerous risk alleles for IgAN that also correlate with the immune response against intestinal pathogens, IgA synthesis within the gut, integrity of the intestinal epithelial barrier, and inflammatory bowel disease (Rehnberg et al., 2021). Interestingly, a cross-sectional study revealed variations in the gut microbiota profile among individuals with progressive IgAN (Kiryluk et al., 2014). While the sensitivity of the gut to diverse mucosal antigens has been documented in IgAN, there is currently no definitive evidence supporting the clinical efficacy of any specific dietary modification (Pei & Guo, 2025). However, there is a proven effect of the targeted-release formulation of budesonide, which releases the active drug at the distal ileum, specifically targeting the Peyer's patches where IgA, and particularly Gd-IgA1, is primarily produced (Barratt, Lafayette, Kristensen, et al., 2023).

Aim of the Thesis

The study was conducted to evaluate the risk of disease progression in patients with IgAN and to analyse B-cell differentiation and the gut microbiome as potential factors in the pathogenesis of the disease.

Tasks of the Thesis

1 To evaluate kidney survival in patients with histologically confirmed IgAN by calculating the risk of a 50 % decline in renal function or progression to ESKD over five years
2 To compare these outcomes with risk predictions using IIgANPT.
3 To investigate alterations in B-cell differentiation in IgAN patients.
4 To compare the composition and functional pathways of the gut microbiome in IgAN patients and healthy individuals.

Hypotheses of the Thesis

1 IIgANPT accurately predicts the risk of disease progression in patients with IgAN and can be effectively applied in the Latvian population.
2 Alterations in B cell differentiation and gut microbiome composition contribute to the pathogenesis of IgAN.

Novelty of the Thesis

At present, the diagnosis of IgAN requires kidney biopsy and immunofluorescence analysis of the kidney tissue. In Latvia, the ability to diagnose this disease has been available since 2013. It is well recognised that the distribution and clinical presentation of IgAN vary across regions and ethnicities. Prior to this study, no published data existed on the course, clinical manifestations, or prognosis of glomerulonephritis specific to the Latvian population. Following the publication of the IIgANPT, which has since been validated in various countries, we evaluated its applicability in our Latvian patient cohort.

The mechanisms responsible for mesangial IgA1 deposition and subsequent renal injury remain incompletely understood. Searching for possible agents involved in the pathogenesis, our study group uncovered the previously unknown B cell activation pathway that is associated with pathogenic IgA secretion – differentiation of IgA-expressing plasmablasts via a CD21+ B cell intermediate, that lacks the classical memory B cell marker CD27, and is enhanced in patients with IgAN. IgA+CD27-CD21+ B cell frequency correlates with serum lipopolysaccharide (LPS) levels, implicating mucosa in their activation. This pathway holds potential for further investigation to identify biomarkers and therapeutic targets in IgAN. These findings can be integrated into the multi-hit pathogenesis model of IgAN.

According to previous studies on gut microbiome changes in IgAN patients, no consistent significant variations in the abundance of specific bacteria have been reported. In our study, butyrate-producing bacteria (*Butyrococcus* and *Agathobacter rectalis*) were less abundant in IgAN patients than in healthy controls, along with a reduced presence of the sulfoquinovose degradation I pathway, in which these bacteria are involved. These findings suggest a potential avenue for further research – specifically, an interventional study to evaluate the effects of butyrate supplementation in IgAN.

When examining microbial community function, we observed increased biosynthesis of nucleosides (adenosine, guanosine, and inosine) in IgAN patients, suggesting a possible link to intestinal inflammation and barrier dysfunction. Gd-IgA1 accounted for a substantial portion of the observed variations in metabolic pathways. Notably, previous studies have not investigated metabolic pathway differences between IgAN progressors and non-progressors. In our study, pathways enriched in patients with progressive kidney function decline were associated with bacterial phospholipid synthesis, suggesting an adaptive process to enhance bacterial survival.

1 Materials and Methods

1.1 Patient characteristics

This study consists of three parts: the first, a retrospective cohort study, focuses on kidney survival analysis and its prediction; the second, a case-control study, addresses B cell differentiation pathways; and the third, a cross-sectional study with an embedded prospective cohort component, examines gut microbiome features in patients with IgA nephropathy. The study structure, including the number of patients involved in each part and the analyses performed, is illustrated in Annex 1. Adults with histologically proven IgAN selected from renal biopsy registry at Pauls Stradins Clinical University Hospital, Latvia were enrolled in the study. This is the only centre for kidney diseases in Latvia that confirms the diagnosis of IgAN in adults; therefore, the IgAN patient cohort is representative of Latvian adults with IgAN. Pathohistological investigation of kidney samples was performed using light microscopy, immunofluorescence, and electron microscopy. Kidney biopsy results were analysed according to revised Oxford classification (MEST-C score): mesangial hypercellularity (M), endocapillary cellularity (E), segmental sclerosis (S), interstitial fibrosis/tubular atrophy (T) and crescents (C) (Trimarchi et al., 2017). The decision to perform the biopsy as well as treatment management were determined by the treating physician based on the specific indications: impaired kidney function or changes in urinalysis.

Renal survival and validation of IIgANPT (Barbour et al., 2019) was studied in adults diagnosed with IgAN from 2013 to 1 November 2019. Kidney survival was defined as having a glomerular filtration rate (GFR) > 15 ml/min /1.73 m^2 within 5 years after the biopsy. Predicted risk was defined as a risk of 50 % decline in eGFR or ESKD calculated by the IIgANPT. Observed risk was a risk of 50 % decline in eGFR or ESKD calculated by the Cox regression model considering the same parameters as in the IIgANPT.

To study gut microbiome characteristics and mechanisms of IgA+ B cell differentiation, IgAN patients and age- and sex-matched healthy volunteers were enrolled from January 2020 till December 2022. The healthy controls (HC) had age-appropriate kidney function, with no active urine sediment and no presence of proteinuria. Exclusion criteria of both group individuals were pregnancy, diabetes mellitus, severe organ dysfunction, acute cardiovascular disease, hepatic diseases, acute or chronic autoimmune or infectious diseases, immunodeficiency, malignancies, alcohol abuse. All participants provided written informed consent.

Medical records were reviewed up to March 2024 to calculate the decrease in eGFR during the follow-up period. Progressors were defined as patients with an eGFR decline of

more than 5 ml/min/1.73 m^2/year, whereas nonprogressors had an eGFR slope of 5 ml/min/1.73 m^2/year or less.

Ethics Committee permission. Retrospective and prospective studies were approved by Clinical Research Ethics Committee of Pauls Stradiņš Clinical University Hospital (Approval No 100118-10L and No 191219-6L).

1.2 Clinical laboratory tests

Serum creatinine, albumin and total cholesterol were measured on Atellica CH (Siemens Healthineers, Erlangen, Germany). eGFR was calculated using the CKD-EPI Creatinine 2009 (in data analysis before 2021) and 2021 Equation. Serum IgA was measured on Atellica NEPH 630 (Siemens Healthineers, Erlangen, Germany). Proteinuria was determined by spot protein-to-creatinine ratio (UPCR). Assessment of protein in urine was performed on Cobas Integra 400 Plus (Roche Diagnostics GmbH, Mannheim, Germany). Red blood cell count in urine was determined on Atellica 1500 automated urinalysis system (Siemens Healthineers, Erlangen, Germany). The complete blood counts were performed on ethylenediaminetetraacetic acid (EDTA)-treated peripheral blood samples using UniCel DxH cellular analysis system (Beckman Coulter, Miami, FL, USA). The Gd-IgA1 level in the serum was measured using ELISA kit (Gd-IgA1 Assay Kit-IBL 30111694, IBL International GmBH, Germany) following the manufacturer's instructions. The samples were diluted 200-fold with the provided EIA buffer, to obtain biomarker levels within the measurement range of the kit (1.56–100 ng/ml). Serum LPS levels were detected by ELISA (MyBioSource MBS702450, San Diego, CA, USA).

1.3 Analysis of the differentiation of IgA+ plasmablasts

Peripheral blood mononuclear cell (PBMC) isolation and serum collection

Peripheral blood was obtained from study participants. Serum from tubes with coagulation activator was isolated by centrifugation and was either used immediately or stored at −80 °C. PBMCs were isolated from heparinised blood by density gradient centrifugation using Histopaque-1077 (Sigma-Aldrich, St. Louis, USA). After washing with complete RPMI-1640 (10 % foetal bovine serum and 1 % penicillin-streptomycin in RPMI-1640), PBMCs were resuspended in freezing media (90 % fetal bovine serum and 10 % dimethyl sulfoxide) and cryopreserved. All laboratory analyses were done in the Joint Laboratory at Pauls Stradiņš Clinical University Hospital (Riga, Latvia).

Immunophenotyping of peripheral blood B cells by flow cytometry

Using antibodies against CD24, CD27, CD38 and IgD we were able to enumerate transitional (CD24hiCD38hi), mature naive (CD24intCD38int), activated (CD24loCD38lo),

and total memory (CD24hiCD38lo) B cells, including class-switched (IgDneg) and unswitched (IgDpos) subsets, double negative (IgDnegCD27neg) B cells, pre-plasmablasts (CD24loCD38hi) and plasmablasts (CD27posCD38hi). We further interrogated IgA, CD21, T-bet, Ki-67 expression in B cell subsets. Briefly, for PBMC viability LIVE/DEAD Fixable Near-IR Dead Cell Stain Kit was used (Invitrogen, MA, USA). Nonspecific staining was prevented with Fc receptor blocking reagent (Miltenyi Biotec, Bergisch Gladbach, Germany). The cells were incubated with antibodies for 40 minutes at 4°C, afterwards unbound antibodies were removed by two washes with flow cytometry staining buffer (2 % fetal bovine serum and 2 mM EDTA in phosphate-buffered solution) and fixed with PBS containing 2 % formaldehyde. For intracellular and transcription factor staining, cells were fixed and permeabilised using the Foxp3/Transcription Factor Staining Buffer Set (00-5523-00, eBioscience) followed by incubation with antibodies diluted in permeabilisation buffer for 50 minutes at 4 °C. Samples were acquired on the Navios EX flow cytometer (Beckman Coulter, Inc., Brea, CA, USA) and analysed with FlowJo software (BD Life Sciences). For the detection of GdIgA1 in B cells, we stained PBMCs with AlexaFluor 488-labelled (ReadyLabel Antibody Labeling Kit R10712, Invitrogen, Waltham, MA, USA) monoclonal antibody [Gd-IgA1 (KM55)-IBL 30117066, IBL Japan, Gunma, Japan] or isotype control (MAB0061, R&D Systems, Minneapolis, MN, USA) for 40 min at 37 °C. To evaluate Gd-IgA1 expression in plasmablasts, cells were permeabilised using the Foxp3/Transcription Factor Staining Buffer Set and stained intracellularly with anti-Gd-IgA1 antibody or isotype control. Both anti-Gd-IgA1 and isotype control were used at a final concentration of 67 µg/ml.

1.4 Gut microbiome analysis

Stool sample collection, microbial deoxyribonucleic acid (DNA) isolation and shot-gun sequencing of DNA libraries. Stool samples were collected in two aliquots using sterile, buffer-free collection tubes. Each participant documented the precise date and time of sample collection. The samples were then aliquoted into cryogenic storage vials and stored at −80 °C until analysis. The extraction of microbial DNA was carried out using the MGISP-960 Automated Sample Preparation System (MGI Tech Co., Ltd., Wuhan, China) and the MagPure Stool DNA LQ Kit (Angen Biotech Co., Ltd., Guangzhou, China). DNA library preparation was performed using the MGIEasy Universal DNA Library Prep Set (MGI Tech Co., Ltd., Wuhan, China) following the manufacturer's instructions. The subsequent sequencing was conducted on the DNBSEQ-G400RS platform using the DNBSEQ-G400RS high-throughput sequencing set (PE 150) (MGI Tech Co., Ltd., Wuhan, China), which provides at least 20 million 150 bp paired-end sequencing reads per sample. The quantity and

quality of the DNA were assessed using a Qubit 2.0 fluorometer (Thermo Fisher Scientific, Waltham, MA, USA) and an Agilent 2100 Bioanalyser system (Agilent Technologies, Santa Clara, CA, USA), respectively.

1.5 Statistical analysis

Statistical analyses were conducted using GraphPad Prism 9 (La Jolla CA, USA), IBM SPSS Statistics 22.0 and 26.0 0 (IBM Corp., USA), and R-Studio version 4.0.1 (R Core Team (2020): R: A language and environment for statistical computing; R Foundation for Statistical Computing, Vienna, Austria. Data distribution was assessed by the Shapiro-Wilk test and normal Q-Q plots. Normal distributed data were expressed as mean ± SD. Not normally distributed data were presented as median and interquartile range. For normally distributed and homogenous data, independent samples t-test was used; when data were not normally distributed, Mann-Whitney U test was used. Spearman's rank correlation test was used to interrogate statistical significance in correlations. Results were considered statistically significant at $p < 0.05$.

Kidney survival was analysed using the Kaplan-Meier method, and statistical comparisons were made using the log-rank test. Episode rates per patient-year were calculated in two patient groups in the five-year analysis: (1) those included in the Kaplan–Meier analysis and (2) Cox regression model.

To compare real patient data with the IIgANPT, the following analyses were performed:

1 Observed risk was calculated using the Cox regression model.
2 Intraclass correlation coefficient was used to assess the strength of agreement between the IIgANPT predictions and the Cox regression results.
3 Differences between predicted and observed risks were calculated and interpreted as follows: a negative difference indicated that the IIgANPT assigned a lower risk than the observed risk; a positive difference indicated that the IIgANPT assigned a higher risk than the observed risk.

For metagenomic shotgun sequencing data read quality evaluation and trimming was done using fastp v0.20.0 (Chen et al., 2018) with default parameters and by retaining only those reads that passed the 100 bp length requirements after the trimming. Host read contamination was controlled by mapping the reads against a Homo sapiens GRCh38 reference genome with Bowtie2 v2.3.5.1 (Langmead & Salzberg, 2012) and removing the mapped reads. Taxonomic classification was performed by using Kracken2 v2.0.8 (Wood et al., 2019) with a confidence parameter set at 0.1 in accordance with the Unified

Human Gastrointestinal Genome (UHGG) (Almeida et al., 2021) collection. Functional profiling was carried out using the HUMAnN 3.0 (Beghini et al., 2021) software.

Statistical analysis for the phylum, genus and species taxonomic levels was performed by using the phyloseq v1.48.0 (McMurdie & Holmes, 2013) microbiome analysis environment. First, we performed frequency and prevalence filtering to exclude taxa that had no counts in any of the samples and samples that had no counts in any of the detected taxa. Alpha diversity indices were calculated using the microbiome v1.26.0 (Lahti & Shetty, 2012–2019) package, which was subsequently used as an input for the Wilcoxon rank sum test in the ggpubr v0.6.0 (Kassambara, 2023) package with Benjamini-Hochberg p-value correction. Sample and group-level taxon proportion plots were produced from proportionally transformed counts using the MicrobiotaProcess v1.16.1 (S. Xu et al., 2023) package. Aitchison's distance was calculated and plotted as a principal component analysis (PCA) plot for taxa passing the 10 % sample prevalence threshold using the MicroViz v0.12.5 (Barnett et al., 2021) package to represent the beta diversity results. Significant covariate detection was performed via the canonical correspondence analysis ordinance method and PERMANOVA test within the MicroViz package, with 99999 permutations. The resulting significant covariates were included in the MaAsLin2 v1.18.0 (Mallick et al., 2021) design formula for the negative binomial analysis method of differentially abundant taxa detection with trimmed mean normalisation applied beforehand, while the default values of the remaining parameters were used, except for increasing the taxon prevalence threshold from 10 % to 33 % in the case-control species level test, to reduce the number of sporadic results. The same analysis methodology was applied to investigate the functional alterations in our experimental group. The default false discovery rate (FDR) threshold in MaAsLin2 is < 0.25, with taxon-level associations below this value considered statistically significant in microbiome studies, requiring further validation (Stewart et al., 2018). Visualisations were created using ggplot2 v3.5.1 (Wickham, 2016) or the previously specified packages.

2 Results

2.1 Kidney survival and its associated clinical and histological risk factors

A total of 105 newly diagnosed IgAN patients were identified between January 2013 and November 2019. Of these, 90.5 % (n = 95) were included in the subsequent kidney survival analysis, while 9.5 % (n = 10) were excluded due to ESKD (eGFR < 15 ml/min/1.73 m²) at the time of biopsy. Demographic and clinical characteristics of the included patients are summarised in Table 2.1. All patients were of white ethnicity and middle-aged, with a mean age of 38.6 ± 11.2 years (range:18–72 years). The majority (40 %) belonged to the 30–39-year age group (Figure 2.1).

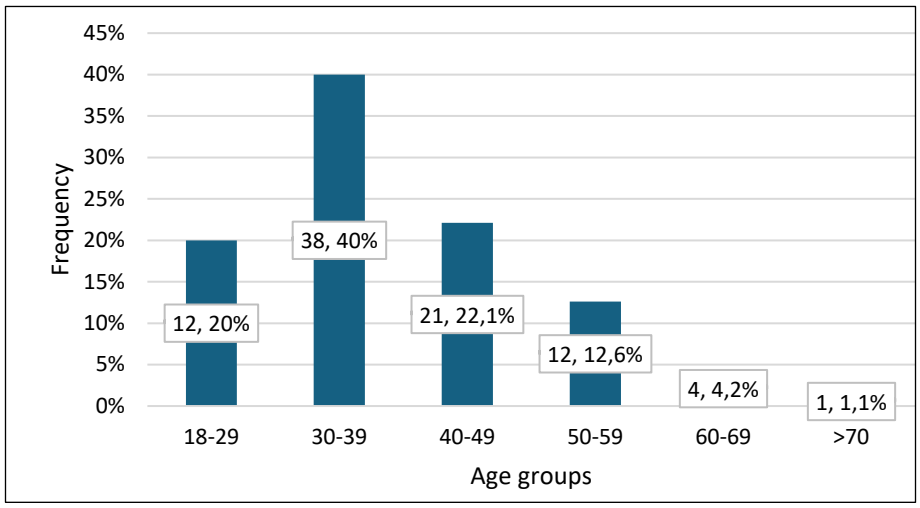

Figure 2.1 **Distribution of IgAN cases by age group**

Nephritic syndrome was the most common manifestation of IgAN, observed in 73.4 % of patients, followed by a combined presentation of nephrotic and nephritic syndrome, characterised by nephrotic-range proteinuria and haematuria (13.8 %), and asymptomatic urinary abnormalities (11.7 %). Nephrotic syndrome was identified in only one patient. Median proteinuria was 1.2 g/g, measured by the UPCR. eGFR ranged from 16 to 130 ml/min/1.73 m², with a median of 56 ml/min/1.73 m². Patients were categorised into different CKD stages based on their eGFR (Figure 2.2). A normal eGFR (> 90 ml/min/1.73 m²) with urinalysis abnormalities was observed in 32 patients (33.7 %). Moderate to severe kidney function loss (eGFR < 60 ml/min/1.73 m²) was present in 47 patients (49.5 %).

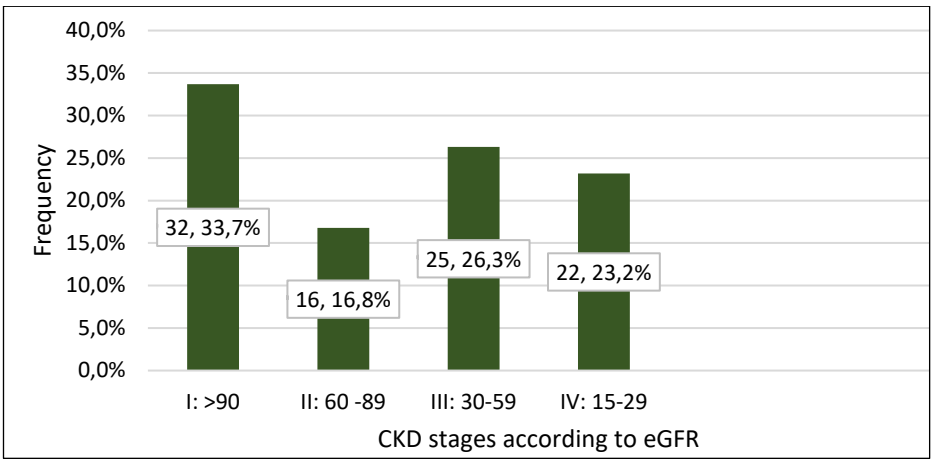

Figure 2.2 **Distribution of IgAN patients by stage of CKD**

On physical examination, hypertension was detected in 56.4 % of patients (defined as SBP ≥ 140 mmHg and/or DBP ≥ 90 mmHg), and 39.6 % of them were using ACEI/ARB at the time of biopsy. In this study cohort, a significant proportion of IgAN patients exhibited mesangial hypercellularity (87.4 %) and segmental glomerulosclerosis (72.6 %). Various degrees of tubular atrophy were identified in 17 (17.9 %) patients.

Table 2.1

Demographic and clinical characteristics of patients included in the kidney survival analysis

Parameters	n (%)
Male	53 (55.8)
Age, years	37 (31–45)
SBP, mmHg	135 (120–150)
DBP, mmHg	80 (71.8–93.0)
GFR at biopsy, ml/min/1.73 m^2	56 (33–98)
Daily proteinuria, g/24 h	1.2 (0.5–2.33)
Oxford classification M1 E1 S1 T1 T2	 83 (87.4) 3 (3.2) 69 (72.6) 11 (11.6) 6 (6.3)
Use of ACEI or ARB at the time of biopsy	37 (38.9)
Immunosuppression at or prior the biopsy	9 (9.5)
Glomerular manifestations Nephritic syndrome Nephrotic syndrome Nephrotic and nephritic syndrome Isolated haematuria Isolated proteinuria	 69 (73.4) 1 (1.1) 13 (13.8) 7 (7.4) 4 (4.3)

Values are shown as frequencies and proportions (%) or median and interquartile range. SBP – systolic blood pressure. DBP – diastolic blood pressure. ACEI – angiotensin-converting enzyme inhibitors. ARB – angiotensin II receptor blockers.

The median follow-up duration was 18 months (ranging from 0 to 60 months). In this study, the overall median kidney survival during the follow-up period (60 months) was not reached; however, the third quartile (Q3) was 24 months. Among the 95 patients included in the analysis, 14 (14.7 %) progressed to ESKD, corresponding to an incidence rate of 0.11 episodes per patient-year. Gender, MEST-T score, and DBP were identified as significant risk factors for reduced kidney survival, while SBP showed a borderline statistically significant association ($p = 0.059$).

Women had a longer kidney survival time (exceeding 60 months) compared to men (58 months). A log-rank test was performed to assess differences in survival distribution between genders; $\chi2(1) = 4.03$, $p = 0.045$ (Figure 2.3).

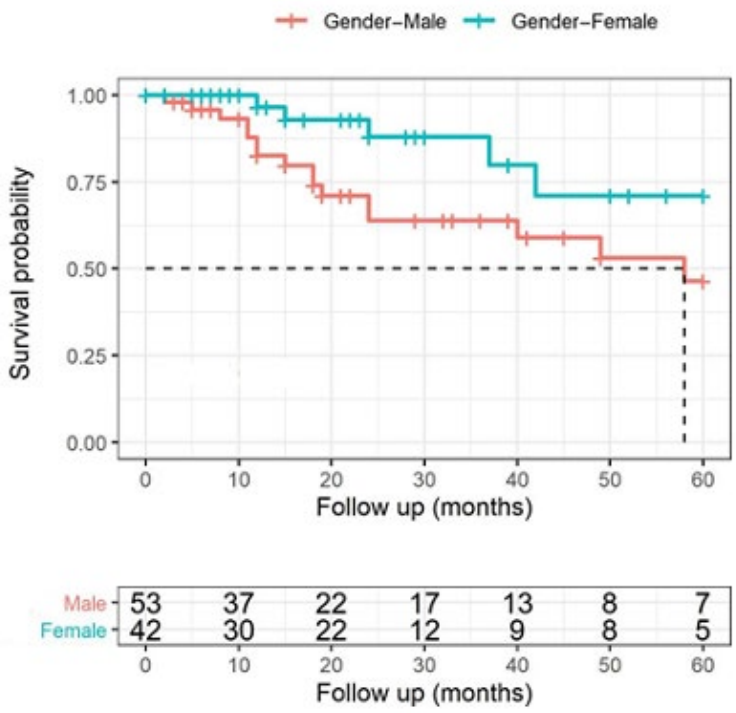

Figure 2.3 **Cumulative kidney-survival rates categorised by gender**

Men had worse kidney survival rates than women during the follow-up period. *p=0.045

The analysis of kidney survival based on to the MEST score showed that patients with a MEST T0 score had a longer median kidney survival time throughout the follow-up period (60 months) compared to those with T1 (40 months) and T2 (18 months). A statistically significant difference in kidney survival distribution was observed between T0 and T1 scores ($\chi2(2) = 9.09$, $p = 0.01$; Figure 2.4). T1 also demonstrated a tendency toward better overall survival compared to T2 ($\chi2$ for trends = 8.80, $p = 0.003$).

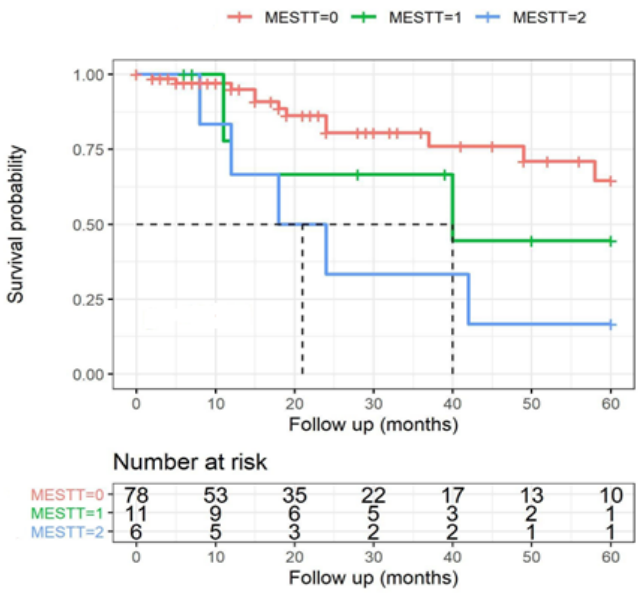

Figure 2.4 **Cumulative kidney survival rates categorised by tubular atrophy/ interstitial fibrosis**

Kidney survival according to the MEST T score revealed that patients with MEST T2 have a poorer prognosis compared to those with T1 and T0. *p=0.01

Participants with a DBP less than 99 mmHg had a longer median kidney survival of 60 months compared to those with DBP levels of 100–109 mmHg (40 months) and those with DBP greater than 110 mmHg (24 months). A statistically significant difference in survival distribution was observed between the DBP categories ($\chi2(4) = 11.46$, $p = 0.022$; Figure 2.5), indicating an association between higher blood pressure and worse kidney survival ($\chi2$ for trend = 9.21, $p = 0.002$).

In this study, survival distribution for age, proteinuria, use of ACEI/ARB at the time of biopsy, the use of immunosuppression at or prior to biopsy, and MEST M, E, and S scores were not statistically significantly affecting kidney survival.

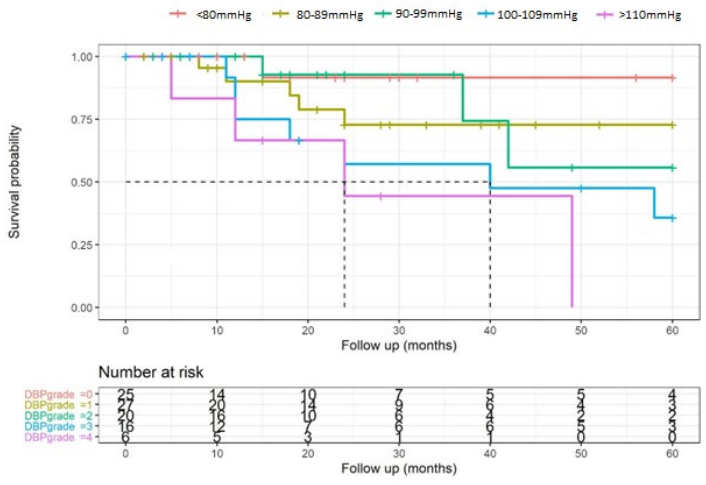

Figure 2.5 **Cumulative kidney survival rates categorised by diastolic blood pressure**

Kidney survival rate is better in patients with lower DBP. *p=0.022

DBP grades 0: < 80 mmHg; grade 1: 80–89 mmHg; grade 2: 90–99 mmHg, grade 3: 100–109 mmHg, grade 4: > 110 mmHg

2.2 Prediction of kidney function decline by Cox regression and the International IgAN Prediction Tool

A total of 68 patients were included in the Cox regression analysis, of whom 37 were men. The mean patient age was 39.1 ± 12.0 years (ranging from 18 to 72 years). We excluded 27 patients due to missing data (mostly absence of 24-hour proteinuria), required for prognosis calculation using IIgANPT (23 patients) and secondary IgAN (4 patients) related to IgA vasculitis or liver disease. The median follow-up duration for the five-year analysis was 21.5 months (ranging from 0 to 60 months). The event rate (50 % decline in GFR or progression to ESKD) was 0.15 episodes per patient-year over five years.

The analysis of hazard ratios revealed that DBP, MEST-E, and MEST-T were associated with the risk of a 50 % decline in GFR or progression to ESKD (Table 2.2). Each subsequent increase in DBP grade was associated with a 6 % rise in risk. Additionally, the risk increased fourfold when moving from E0 to E1 in the MEST-E score, and more than doubled for each unit increase in the MEST-T score. Conversely, age showed a protective effect, with the risk decreasing by 5 % for each additional year.

Table 2.2

Hazard ratio of various clinical parameters in IgAN patients

Factor	Hazard ratio (95 % confidence interval)	p-value
Age	0.95 (0.91–0.99)	0.023
SBP	0.99 (0.96–1.03)	0.683
DBP	1.06 (1.00–1.12)	0.04
MEST E	4.12 (0.83–20.47)	0.084
MEST T	2.52 (1.38–4.62)	0.003

Further analysis compared the observed and predicted five-year risks using the IIgANPT. The intraclass correlation coefficient (ICC) indicated a moderate level of reliability between predicted and observed risk, with an average-measure ICC of 0.70 (95 % confidence interval: 0.52 to 0.82; $F(67.67) = 3.38$, $p = 0.001$). Most differences between predicted and observed data fell within the range of 0 to 10 % ($n = 33$), with a median difference of 2.54 %, suggesting good reliability of the IIgANPT. While the IIgANPT underestimated risk in 23 patients compared to our estimates, it assigned similar or slightly higher risk in 45 patients. However, the maximum negative and positive differences were 77.35 % and 59.84 %, respectively. A closer examination of these outliers revealed no exceptional features in their disease course or histology.

2.3 B cell activation pathways in IgAN patients

To uncover B cell activation pathways and how peripheral B cell composition may be impacted in patients with IgAN, we recruited 36 patients with IgAN and 19 HCs. Study participants were sex- and age-matched. Both groups had normal and comparable leukocyte and lymphocyte counts. As expected, IgAN patients had higher serum creatinine levels and lower eGFR than HC. IgAN patients represented all four chronic kidney disease stages (from 1 to 4) based on eGFR. The median proteinuria of patients with IgAN was 0.48 g/g (interquartile range 0.26–1.35), 11 patients had moderate proteinuria (1–3 g/g) and only one patient had nephrotic-range proteinuria (> 3 g/g). According to the Oxford classification of IgAN, a frequent histological finding was secondary glomerulosclerosis (69.4 %). Only in rare cases tubular atrophy or crescents in < 25 % of glomeruli were seen. There were no significant differences in body mass index (BMI) between IgAN patients and controls.

We first carried out B cell phenotyping based on CD24, CD27, CD38 and IgD surface expression. This allowed us to enumerate transitional ($CD24^{hi}CD38^{hi}$), mature naive ($CD24^{int}CD38^{int}$), activated ($CD24^{lo}CD38^{lo}$), and total memory ($CD24^{hi}CD38^{lo}$) B cells, including class-switched (IgD-) and unswitched (IgD+) subsets, double negative (IgD-CD27-) B cells, pre-plasmablasts (CD24loCD38hi) and plasmablasts (CD27posCD38hi). We found that IgAN patients had a significant increase in mature naive B cells with a reciprocal decrease in the frequency of total memory B cells (Figure 2.6 a). Frequencies of switched and unswitched memory B cells were comparable (Figure 2.6 b). A total of IgD-CD27- B cells termed double negative (DN) or atypical memory B cells, that has been recently described as the precursors of autoantibody-producing plasmablasts, were comparable to plasmablasts in patients with IgAN and HC (Figure 2.6 c).

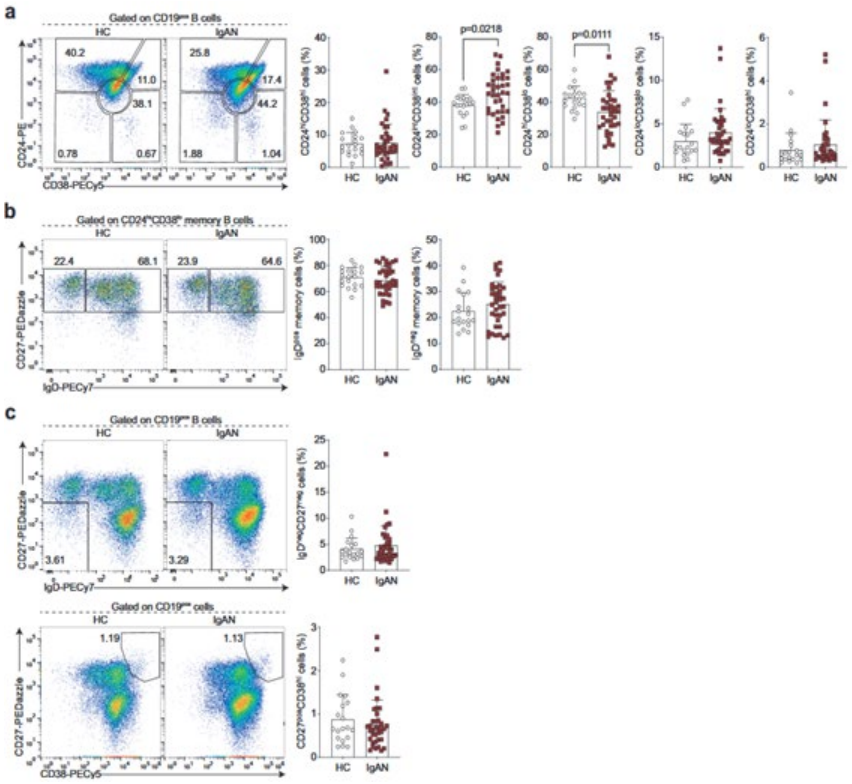

Figure 2.6 **IgAN-associated changes in the peripheral B cell landscape**

Representative flow cytometry plots and summary bar charts demonstrating (a) the frequencies of transitional (CD24hiCD38hi), mature (CD24intCD38int), memory (CD24hiCD38lo), activated B cells (CD24loCD38lo) and pre-plasmablasts (CD24loCD38hi), (b) the distribution of memory B cells into IgD+ unswitched and IgD- class-switched subsets, (c) the frequencies of total double negative (DN; $IgD^{-}CD27^{-}$) B cells and plasmablasts (CD27+CD38hi) in IgAN patients and healthy controls. Data are mean ± SD and each circle/square represents a study participant.

The cellular origin and pathway that gives rise to IgA-producing B cells in IgAN is unknown. We wanted to determine whether systemic changes in the activation and differentiation of IgA-expressing B cells could be detected in IgAN patients. Among B cells, the frequency of IgA-expressing classical memory (CD27+) B cells was similar between IgAN patients and HC (Figure 2.7 a). However, we noted that in addition to CD27 expressing B cells, there was a smaller population of IgA class-switched B cells that lacked CD27 expression, which was particularly pronounced in IgAN patients. Indeed, there was a significant expansion of these IgA-expressing $CD27^{-}$ B cells in patients with IgAN (Figure 2.7 a). We also detected a significantly higher frequency of IgA class-switched antibody-secreting cells (ASC) in IgAN patients compared to controls (Figure 2.7 b). Supporting a lineage relationship between IgA-expressing plasmablasts and IgA-expressing $CD27^{-}$ B cells, we found a correlation between these two subsets (Figure 2.7 c).

We next wanted to address whether the IgA-expressing B cells were indeed expressing Gd-IgA1. We found that $IgA+CD27^{-}$ B cells co-expressed Gd-IgA1 (Figure 2.7 d). Reciprocally, in IgAN patients the majority of all Gd-IgA1+ B cells were $CD27^{-}$ (Figure 2.7 e and f). IgA+ plasmablasts also expressed high levels of Gd-IgA1 (Figue 2.7 g). Finally,

implicating the IgA-expressing plasmablast as a potential functional contributor to pathogenesis, we observed a correlation between IgA+ plasmablasts and circulating IgA levels (Figure 2.7 h). Nevertheless, despite the correlation between IgA and Gd-IgA1, we did not find a relationship between IgA+ plasmablasts and serum Gd-IgA1 levels (Figure 2.7 i).

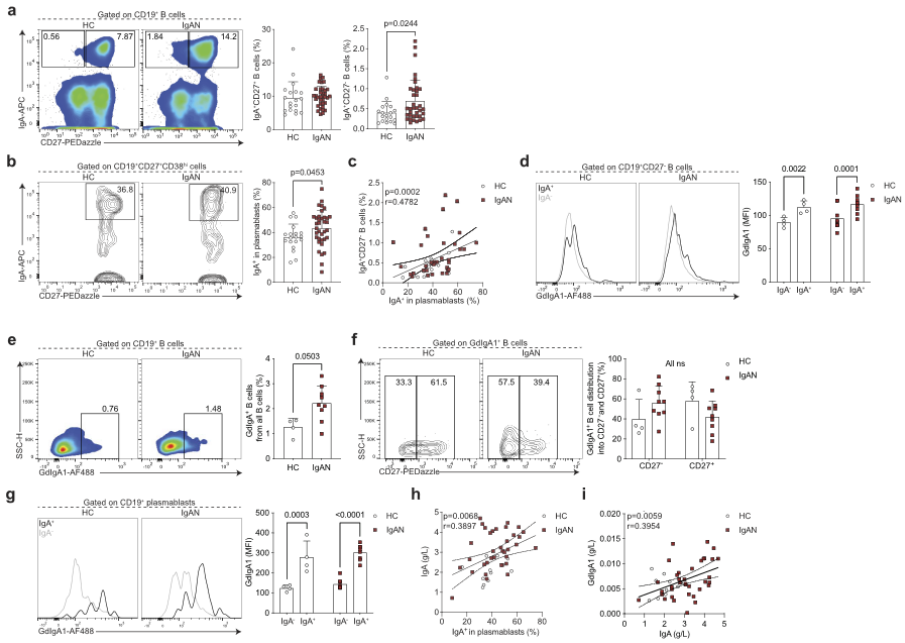

Figure 2.7 **Enhanced differentiation of IgA$^+$ CD27$^-$ B cells and IgA$^+$ plasmablasts in IgAN**

Representative flow cytometry plots and summary bar charts demonstrating the frequencies of (a) IgA+ CD27+ and IgA+CD27$^-$ B cells, and (b) IgA+ plasmablasts, (c) linear regression analysis of IgA+CD27$^-$ B cells versus IgA+ plasmablasts, and (d) representative flow cytometry histograms and summary bar charts demonstrating the median fluorescence intensity of Gd-IgA1 in IgA+ and IgA− CD19+CD27$^-$ B cells. (e, f) Representative flow cytometry plots and summary bar charts demonstrating the frequencies of (e) GdIgA1+ B cells and (f) the distribution of Gd-IgA1+ B cells into CD27$^-$ and CD27+ subsets. (g) Representative flow cytometry histograms and summary bar charts demonstrating the median fluorescence intensity of Gd-IgA1 in IgA+ and IgA− plasmablasts. (h, i) Linear regression analysis of (h) serum IgA levels versus IgA+ plasmablasts and (i) serum Gd-IgA1 versus serum IgA levels in IgAN patients and HC. Data are mean ± standard deviation.

CD27$^-$ antigen-experienced B cells comprise two subsets, termed double negative (DN) 1 and 2. DN1 cells are defined by their expression of CD21 and CXCR5, while DN2 B cells lack CD21 and CXCR5 expression and instead express CD11c and are transcriptionally regulated by T-bet. Based on their transcriptional signatures these two subsets of B cells arise from different activation pathways (Jenks et al., 2018). While DN2 B cells arise through extrafollicular B cell activation, DN1 B cells represent precursors of classical memory B cells that have recently emerged from the germinal centre reaction (and have not yet upregulated CD27). Of note, germinal centres are the microanatomical structures that allow the evolution (by somatic hypermutation of antibody-encoding genes) and selection (affinity maturation) of B cells that enable the production of high-affinity antibodies. The understanding of which pathway B cells are activated through can elucidate

factors that regulate the response (e. g. T cell help) or properties of the compartment (e. g. longevity) (Elsner & Shlomchik, 2020). We found that the IgA−CD27+ B cells were phenotypically CD21^{hi} and T-bet^{lo} corresponding to DN1 phenotype (Figure 2.8 a and b), suggesting they may indeed be the precursors of IgA+CD27+ classical memory B cells.

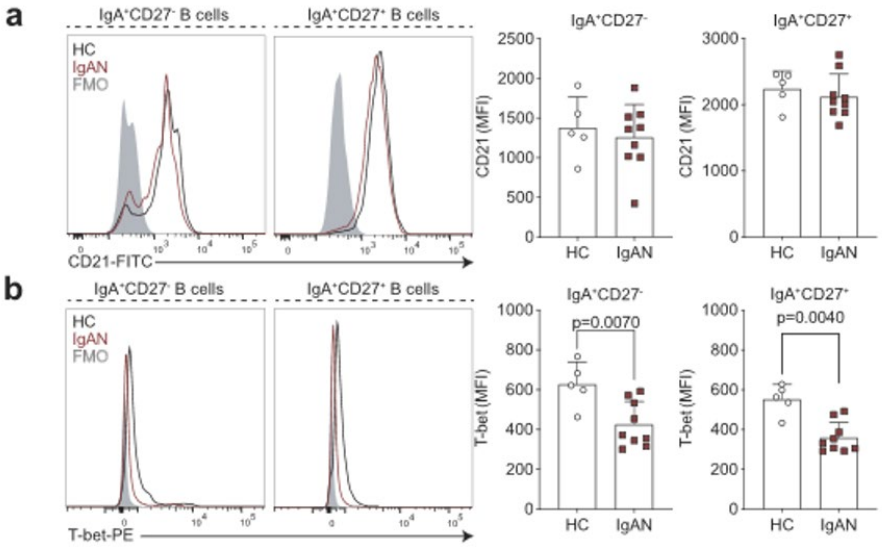

Figure 2.8 **IgA^{+}CD27^{-} B cells are phenotypically CD21^{+}T-bet^{-}**

Representative flow cytometry histograms and summary bar charts demonstrating the median fluorescence intensity of CD21 (a) and T-bet (b) in IgA^{+}CD27^{-} and IgA^{+}CD27^{+} B cells.

Finally, we wanted to explore the mucosal–kidney axis in relation to B cell activation in IgAN and ask if previously reported perturbations at mucosal surfaces were linked to this DN1 B cell differentiation pathway. LPS is known not only to influence B cell class-switching to IgA (Cerutti, 2008), but is also used as a surrogate marker of dysbiosis and gut permeability (Mohr et al., 2022). LPS was significantly elevated in the serum of IgAN patients compared with HC (Figure 2.9 a). We further found that IgA-expressing CD27^{-} B cells correlated with serum LPS levels (Figure 2.9 b). This suggests LPS may either directly drive their expansion/class-switching or that the observed correlation is because both increased LPS and IgA^{+}CD27^{-} B cells are a consequence of mucosal dysbiosis/reduced barrier function, which contributes to IgA-expressing plasmablast differentiation. Finally, we wanted to ask how the expansion of IgA^{+} CD27^{-} B cells related to clinical features of IgAN. We found that specifically in patients with reduced kidney function (eGFR < 90 ml/min) there was an inverse correlation between eGFR and the frequency of IgA^{+}CD27^{-} B cells (Figure 2.9.c).

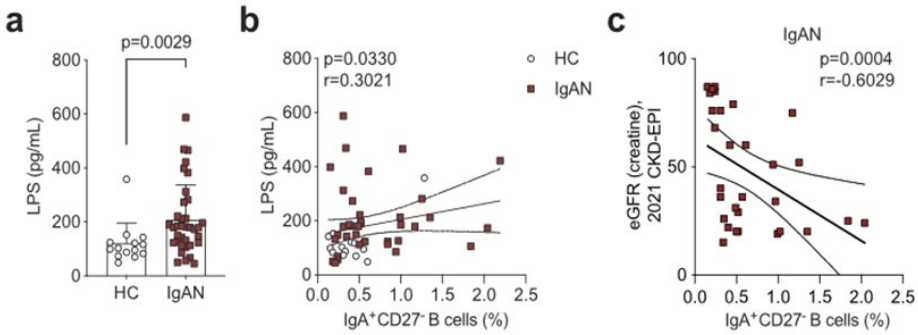

Figure 2.9 **Serum lipopolysaccharides correlation with IgA^{+}CD27^{-} B cell frequency**

(a) Serum LPS levels in IgAN patients and HC (b) linear regression analysis of serum LPS levels versus IgA^{+}CD27^{-} B cells in IgAN patients and HC (c) Linear regression analysis of eGFR versus IgA^{+}CD27^{-} B cells in IgAN patients. Data are mean ± standard deviation and each circle/square represents a study participant.

2.4 Characteristics of gut microbiome composition in IgAN patients

Forty-eight patients with IgAN and twenty-three healthy controls were enrolled in the study for gut microbiome analysis. The study participants were sex- and age-matched, with more than 60 % being men, and ages ranging from 22 to 65 years. Both groups had a similar median BMI of 26 kg/m². As expected, serum creatinine levels were higher in patients with IgAN than in healthy controls. The distribution of IgAN patients across CKD stages was approximately 20 %, with the majority in the CKD stage 1 group (33.3 %). According to the pathological Oxford classification, approximately 70 % of IgAN patients had mesangial hypercellularity (M1) and segmental glomerulosclerosis (S1) findings in their biopsy results. Patients had mild proteinuria, with a median UPCR of 0.349 g/g. Gd-IgA1 levels were greater in IgAN patients than in healthy individuals (p=0.02).

To evaluate the IgAN-related alterations in the gut microbiome profiles, we compared the shotgun sequencing-derived gut microbiome profiles of faecal samples from IgAN patients (n = 48) with those of samples collected from healthy controls (n = 23). We observed no statistically significant differences in alpha diversities estimated by several common indices between the interest groups. In addition, no significant difference in the intersample variability in the microbial community composition among the analysed samples between the case and control groups was observed.

Prevotella was the most prevalent genus in both IgAN patients (7.57 %) and controls (9.27 %), with *Faecalibacterium* (IgAN = 6.71 %, controls = 8.11 %) and *Blautia* (IgAN = 6.73 %, controls = 7.02 %) also among the most common genera. Notably, *Bacteroides* and *Bifidobacterium* were more abundant in IgAN patients than in controls (IgAN = 4.99 % and 2.84 %, controls = 4.56 % and 1.85 %). *Prevotella sp00900557255* (IgAN = 2.95 %, controls = 4.34 %), *Fusicatenibacter saccharivorans* (IgAN = 2.53 %,

controls = 2.58 %), and *Phocaeicola dorei* (IgAN = 2.51 % and controls = 2.28 %) were the three most abundant species in both groups.

Differential abundance analysis at the species level revealed 371 differentially abundant taxa (false discovery rate (FDR) < 0.25) between the IgAN patients and healthy controls, with *Absicoccus sp000434355* (coef. = 3.69, FDR = 3.53E-13), *Bacteroides ndongoniae* (coef. = 3.28, FDR = 4.59E-08), *Akkermansia muciniphila C* (coef. = 2.76, FDR = 1.66E-03) showing higher abundance, while *Eubacterium R sp000433975* (coef. = −3.28, FDR = 9.09E-07), and *CAG:462 sp900291465* (coef. = −3.23, FDR = 4.90E-09), *Olsenella E sp900540955* (coef. = −2.98, FDR = 1.75E-03) and *Butyricicoccus A sp002395695* (coef. = −2.52, FDR = 5.00E-08) had a lower abundance in IgAN patients (Figure 2.10.a and b).

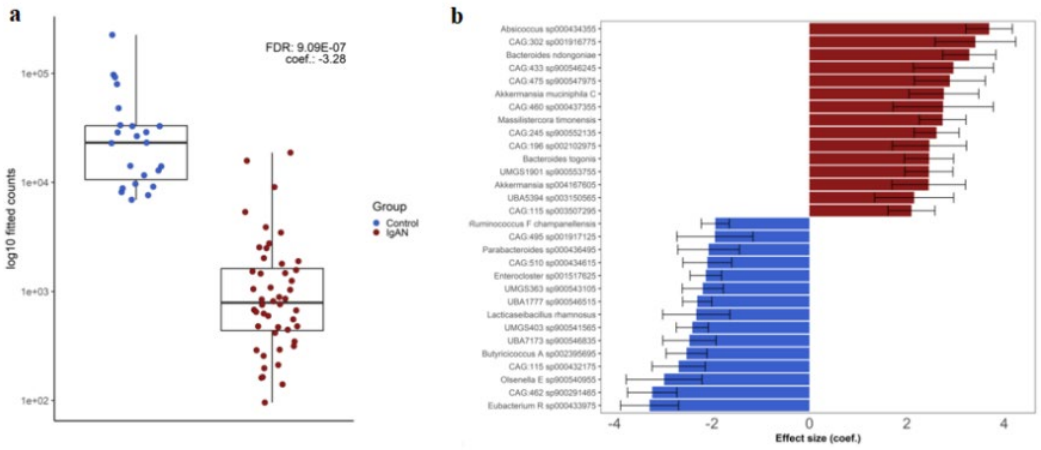

Figure 2.10. **Alterations in the gut microbiome in IgAN patients and healthy individuals**

(a) Relative abundance of Eubacterium R sp000433975 in control subjects (blue) and IgAN patients (red). Boxplots show the median, 25th, and 75th percentiles and outliers. (b) Bar plot representing the effect size (logFC) of the top 20 differentially abundant species between control subjects and IgAN patients. A positive coefficient (red) represents taxa with increased abundance in the IgAN patients, and a negative coefficient (blue) represents taxa in the control patients.

The functional consequences derived from gene mapping were supported by comparative MetaCyc metabolic pathway profiling between the gut metagenomic sample pools of control subjects and IgAN patients, revealing 34 significantly differentially abundant gut microbiome functional pathways. 4-Hydroxyphenylacetate degradation was the most enriched pathway in healthy controls compared with that in IgAN patients (coef. = −3.97, FDR = 1.00E-01), followed by the superpathway of lipopolysaccharide biosynthesis (coef. = −3.53, FDR = 2.24E-01) and the sulfoquinovose degradation I pathway (coef. = −3.51, FDR = 1.43E-01). However, multiple nucleotide- and nucleoside-biosynthesis-related pathways (including adenosine, guanosine, inosine, and pyrimidine biosynthesis) were more prominent in IgAN patients, as was glycolysis from glucose-6-phosphate (Figure 2.11).

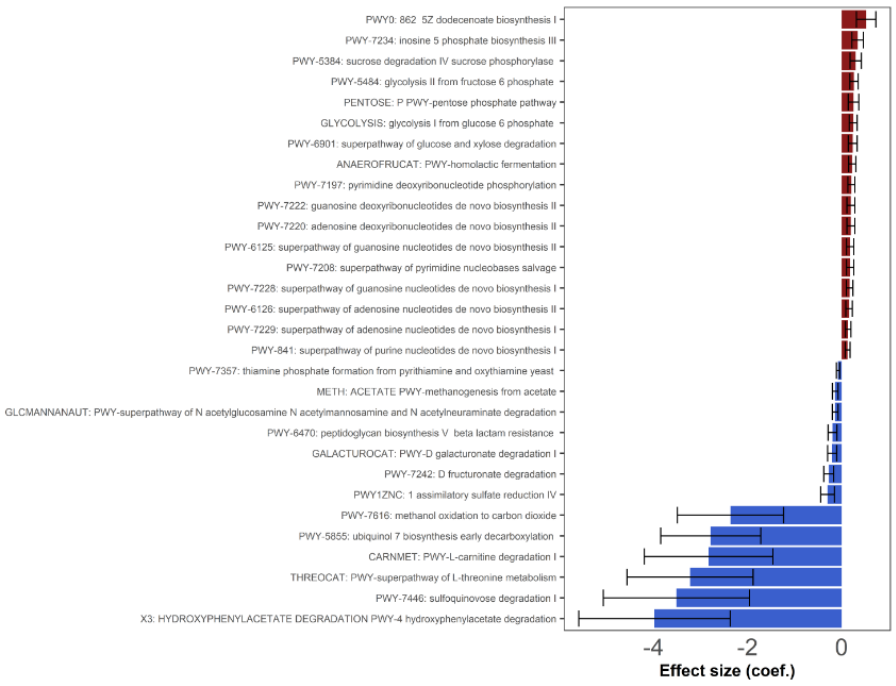

Figure 2.11. **Metabolic differential pathways in IgAN patients and healthy individuals**

The effect size is expressed as a coefficient with positive values for pathways enriched in IgAN patients, while negative values correspond to pathways enriched in control subjects.

Surprisingly, Gd-IgA1 accounted for a greater portion of the observed variations in metabolic pathways (PERMANOVA $R^2 = 0.061$, $p = 0.001$). This influence was greater than that attributed to the eGFR ($R^2 = 0.039$, $p = 0.015$) or BMI ($R^2 = 0.036$, $p = 0.02$).

Next, we aimed to assess the potential differences in the gut microbiome composition by focusing solely on the patient group. We retrospectively stratified the patients into two groups based on their disease progression status: 23 were progressors with an eGFR decrease of more than 5 ml/min per year, and 23 were nonprogressors. Two patients lacked follow-up eGFR data and were excluded from further analysis. The mean follow-up time was 24 months (ranging from 2 to 43 months), with a mean eGFR reduction of 5.8 ml/min/year (ranging from a decline of 30 ml/min/year to an improvement in kidney function by 9 ml/min/year). There was no statistically significant difference in the alpha diversity metrics between the two groups.

Nevertheless, distinct beta diversity clustering was observed between the two groups according to the PERMANOVA test ($R^2 = 0.03$; $p = 0.04$), with notably greater dispersion in progressors. While *Prevotella, Faecalibacterium*, and *Blautia* were the most prevalent genera in both groups, the order of abundance differed between them. In progressors, *Prevotella* was the most abundant genus (9.48 %), followed by *Blautia* (6.50 %) and *Faecalibacterium* (6.12 %), whereas *Faecalibacterium* (7.33 %) was the most common genus in nonprogressors. At the species level, *Prevotella sp00900557255* was the most abundant in progressors, with *Phocaeicola dorei* and *Fusicatenibacter saccharivorans* also prevalent. Among

the nonprogressors, *Agathobacter rectalis* was the most abundant species (2.67 %), followed by *Fusicatenibacter saccharivorans* (2.18 %) and *Phocaeicola dorei* (2.02 %).

The differential abundance analysis at the species level comparing the gut microbiome compositions of progressors and nonprogressors revealed statistically significant differences in 455 taxa. Notably, *Staphylococcus hominis* (coef. = −8.39, FDR = 5.31E-02) and *UBA7173 sp900548705* (coef. = −6.50, FDR = 4.18E-03) were significantly more abundant in nonprogressors, whereas *Dialister hominis* (coef. = 6.38, FDR = 1.85E-08) was significantly more abundant in progressors (Figure 2.12). Among the 455 progression-related taxa, 69 (9 %) showed differential abundance also in the comparison of controls versus IgAN patients (e. g. *Akkermansia sp004167605, Dialister hominis*).

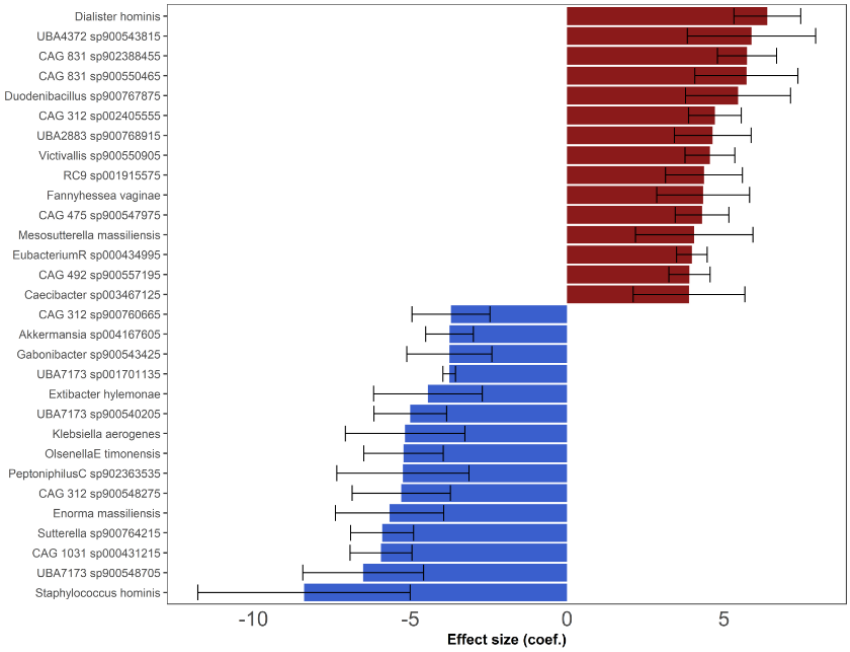

Figure 2.12. **Bar plot representing the effect size (logFC) of the top 20 differentially abundant species between IgAN progressors and nonprogressors**

A positive coefficient (red) represents taxa with increased abundance in the progressor group, and a negative coefficient (blue) represents taxa with increased abundance in the nonprogressors group.

Differential pathway analysis between nonprogressors and progressors revealed 21 metabolic pathways with the N-acetyl D glucosamine biosynthesis II pathway (coef. = −4.64, FDR = 1.27E-01), showing the strongest enrichment in nonprogressors. Progressors exhibited more active isopropanol biosynthesis (coef. = 1.08, FDR = 1.67E-1), followed by biotin biosynthesis II (coef. = 0.52, FDR = 2.28E-1) and phospholipid biosynthesis (Figure 2.13). Consistent with the case-control comparison, Gd-IgA1 accounted for a larger proportion of the observed variations in metabolic pathways (PERMANOVA $R^2 = 0.06$, $p = 0.018$) specifically among IgAN patients. Furthermore, serum Gd-IgA1 levels in IgAN patients were significantly associated with the abundance of 88 metabolic pathways, including 57 positively

associated pathways – such as phospholipid remodeling in yeast (coef. = 1.97; FDR = 1.17E-01) – and 31 negatively associated pathways, such as the superpathway of UDP-N-acetylglucosamine-derived O-antigen building blocks biosynthesis (coef. = −0.69; FDR = 4.33E-29) or creatinine degradation I (coef. = −0.67; FDR = 3.03E-54).

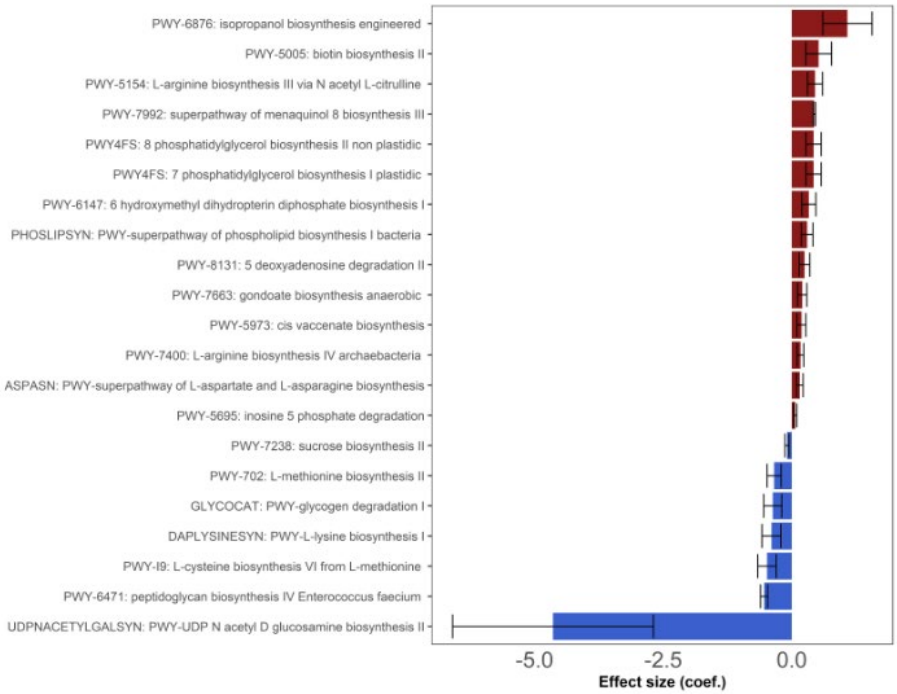

Figure 2.13 **Bar plot of MetaCyc metabolic differential pathways**

The effect size is expressed as a coefficient with positive values for pathways enriched in IgAN progressors and negative values for nonprogressors-related pathways

3 Discussion

The present work provides evidence on risk factors for kidney survival over a five-year period. The IIgANPT was applied to the study population, and the observed and predicted risks were similar, indicating that this tool can be effectively used in the Latvian population. Our results reveal that dysregulation of mucosal immunity drives increased naïve B cell activation in germinal centres, giving rise to $IgA^{+}CD27^{-}CD21^{+}$ B cells and subsequently to IgA-producing plasmablasts. The gut microbiome of patients with IgA nephropathy was analysed to identify possible mechanisms: these patients exhibited a reduction in butyrate-producing bacteria, and functional profiling indicated signs of immune activation and inflammation.

The diagnosis of IgAN in Latvia became possible after 2013, following the initiation of collaboration with the Vilnius Pathology Centre in Vilnius, Lithuania. This partnership enabled the analysis of kidney biopsies using the immunofluorescence method, where the detection of positive IgA deposits in biopsy material confirms the diagnosis. IgAN can present in heterogeneous clinicopathological forms, ranging from asymptomatic urinalysis abnormalities to rapidly progressive glomerulonephritis. Across all discussed above IgAN patient cohorts, a male predominance is observed, with a median age of 40 years, and histological findings commonly showing mesangial hypercellularity and segmental glomerulosclerosis. Patients typically present with nephritic syndrome – characterised by mild to moderate proteinuria – or a nephritic-nephrotic syndrome, often accompanied by progressive glomerulosclerosis, which naturally affects disease prognosis. Approximately 20 % of patients diagnosed with IgAN at Pauls Stradiņš Clinical University Hospital initiated kidney replacement therapy on average 11 months after diagnosis.

The five-year kidney survival time was 57 % in our study group, while the Japanese study of 30-year analysis of kidney survival (n = 1012) showed that five-year kidney survival was more than 90 % (Moriyama et al., 2014). Another retrospective study on kidney survival in IgAN patients analysed long-term outcomes across four cohorts from different countries and three continents. The 10-year kidney survival rates reported were 95.7 % in Helsinki (Finland), 87.0 % in Sydney (Australia), 63.9 % in Glasgow (United Kingdom), and 61.6 % in Toronto (Canada). Additionally, five-year survival rates were 98 % in Helsinki, 95 % in Sydney, and 79 % in both Glasgow and Toronto, as demonstrated by survival curve analysis (Geddes et al., 2003). When comparing our findings to those of the Japanese and tricontinental studies, it appears that the disease course in Latvian patients is more aggressive, with a faster progression to ESKD. Differences in kidney biopsy indications across countries can contribute to this observation. In Japan, kidney biopsies are routinely performed in all patients with

suspected glomerulonephritis. In contrast, in Latvia, urinalysis is not routinely performed in the general population. As a result, many cases remain undiagnosed in time, and individuals often do not consult general practitioners until noticeable symptoms appear. Biopsies are typically conducted only when additional kidney manifestations are present, such as proteinuria, hypertension, or reduced GFR. Patients presenting with isolated haematuria are often not referred for biopsy. IgAN progression may vary by geographic region, proving genetic influence on the course of the disease. The genome-wide association studies have identified over 30 risk loci that may contribute to the pathogenesis of IgAN by affecting the dysregulation of mucosal innate immunity, immune cell proliferation, production of Gd-IgA1, formation of autoantibodies against Gd-IgA1, and activation of compliment system (Xu et al., 2023). A genetic risk score derived from replicated genome-wide association studies loci is highest among Asian populations, intermediate in Europeans, and lowest in Africans, reflecting the known global differences in IgAN prevalence. Notably, the genetic risk score also revealed an unexpectedly higher prevalence of IgAN-related kidney failure in Northern Europe (Kiryluk et al., 2013). Alongside genetic predisposition, there is also evidence of a subtly dysregulated mucosal immune response to antigens in IgAN, as reflected by alterations in gut permeability. Dietary habits, which differ between sexes and across ethnic groups, may also play a role in disease pathogenesis and further prognosis.

Until 2019, there was no validated tool to predict IgAN progression. The treatment decision was based on patient clinicopathologic features; however, as mentioned in the authors' publication, clinical trials suggested that 33 % of patients who did not meet clinical-treatment criteria but had high MEST scores did not receive treatment and experienced a decrease of kidney function, and more than 75 % of patients with low-risk nonprogressive disease were unnecessarily treated. The study population of "evaluating a new international risk-prediction tool in IgA nephropathy" was patients from multiethnic cohorts of adults with biopsy-proven IgAN, and it included patients from Oxford, North American, and VALIGA studies. In VALIGA study, patients from 53 centres in 13 countries were enrolled, and it included only one centre from the Baltic States (Estonia, Tartu) two centres from Scandinavian countries (Sweden), but many centres from Italy; this could indicate that the study population was nonhomogeneous (Barbour et al., 2019; Coppo et al., 2014). Considering that the course of IgAN may vary across different geographical regions, and that the Latvian population may differ from the general populations of Central and Southern Europe, it was important to clarify the disease course specifically within the Latvian population.

Our study focused on actual kidney survival analysis and validation of the IIgANPT in study population. To our knowledge, this was the first study in a European population to compare predicted and observed risks of kidney disease progression since the IIgANPT became available online, followed later by analyses in Greek, Norwegian and French populations (Bon et al., 2023; Haaskjold et al., 2023; Papasotiriou et al., 2022).

In our study, the statistically significant factors affecting kidney survival were gender, MEST-T score, and diastolic blood pressure. Patients with T0 had a median kidney survival time longer than five years; those with T1 had a median survival of 40 months, while patients with T2 had the shortest survival – 18 months. The study and secondary analysis of the STOP-IgAN study also showed that T scores, with no effect modification by age, were associated with lower GFR and worse kidney outcomes (Coppo et al., 2020; Schimpf et al., 2018). Several studies indicated that hypertension prevalence in IgAN patients may vary between 19 % and 53 % at the time of kidney biopsy (Nagy et al., 2005). A large, multi-centre study from China found an overall hypertension prevalence of 63.3 % among 1055 IgAN patients (Zheng et al., 2018). In our study group, 57.3 % (n = 59) of patients had hypertension defined as BP ≥ 140/90 mmHg, yet only 22 were using ACEI/ARB at the time of biopsy. This may be explained by late referral to a nephrologist in the absence of other clinical symptoms, or by caution in prescribing these medications to patients with low GFR. In this study, we found that the blood pressure affects kidney survival; patients with lower blood pressure had longer kidney survival. Zheng *et al*. supports a benefit of intensive control of BP < 130/80 mmHg for patients with proteinuria ≥ 1 g/d (Zheng et al., 2018). If the patient exhibits proteinuria exceeding 0.5 g/d, it is recommended to initiate therapy with either an ACEI or an ARB, regardless of whether hypertension is present (Kidney Disease: Improving Global Outcomes Glomerular Diseases Work, 2021).

Gender affected kidney survival, with women having longer kidney survival than men, and there were differences between predicted and observed data; for females, predicted and observed risks were more similar compared with those for males. Men tend to have poorer prognosis than women in IgAN mainly because male patients often present with worse clinical and pathological features at diagnosis: lower eGFR, greater proteinuria, higher prevalence of hypertension, hypertriglyceridemia, and hyperuricemia, more severe histopathological damage, including segmental sclerosis and tubular atrophy/interstitial fibrosis, higher proportion of global glomerulosclerosis (Deng et al., 2018).

In this study, we found that the predicted and observed risks of a 50 % decline in GFR or progression to ESKD were comparable. Furthermore, the five-year analysis showed a moderate concordance between predicted and actual outcomes, supporting the reliability of

the IIgANPT for use in the Latvian population. Other external validation studies of the prediction tool conducted in Norwegian, Chinese, and Chinese Argentinian cohorts also demonstrated good discrimination and model fit overall. However, in the Chinese Argentinian cohort, the full model (including race) overestimated the risk of progression over a 3-year period (Zhang et al., 2020). In an Indian cohort, the tool showed reasonable discriminatory ability but consistently underestimated risk across all groups (Bagchi et al., 2022). In an increasingly multicultural world, where defining ethnicity is complex, risk stratification based on genetic profiles rather than self-reported ethnicity may offer a more precise approach to predicting outcomes.

This shift toward genetic profiling aligns with growing insights into the molecular and immunological underpinnings of IgAN. Current concept of the pathogenesis of IgAN has been referred to as the "multi-hit" hypothesis (Scionti et al., 2022), and advances have been made particularly in uncovering the mechanisms operating within the kidney that contribute to organ damage. These include the dissection of how immune complexes containing IgA bind to mesangial cells, triggering proliferation and increased synthesis of extracellular matrix components as well as the role of the CD89 in regulating tissue damage (Launay et al., 2000). However, these mechanistic insights are unlikely to lead to major therapeutic breakthroughs, as they reflect processes that occur after B cell tolerance has already been broken.

Our findings reveal alterations in the B cell compartment among patients with IgAN, notably an expansion of naïve B cells and a reduction in total memory B cells. Similar B cell patterns are characteristic of systemic autoimmune diseases such as systemic sclerosis, rheumatoid arthritis (Bugatti et al., 2014; Sato et al., 2004). This observation is particularly significant because IgAN is considered an organ-specific autoimmune disease, and these data suggest that systemic immunity is dysregulated beyond previously characterised mucosal immune abnormalities. However, we did not observe an expansion of total double-negative (DN) B cells, which is typically associated with more severe systemic autoimmune and inflammatory phenotypes. Determining whether the systemic alterations in the overall B cell landscape observed in this study are a cause of IgAN or a consequence of autoimmunity-related inflammation or bystander effects remains an important question.

As the source of pathogenic Gd-IgA1 antibodies, B cells are a promising target in IgAN, but B cell activation and differentiation pathways that lead to pathogenic IgA production remain uncharacterised. Understanding how B cells are affected and become activated is important for the complete understanding of IgAN pathogenesis, prognosis, and treatment. Here we provide mechanistic insight into the early steps of IgAN pathogenesis by uncovering that IgA-expressing B cells that lack the classical memory marker CD27, but

express CD21 are expanded in patients with IgAN and appear to be the cellular precursors of IgA-producing plasmablasts. Our findings indicate that these ASC precursors likely originate from active germinal centres, suggesting a continuous production of pathogenic cells. This points to an ongoing process rather than a predominant contribution from memory B cells or plasmablasts formed earlier. DN1 B cells have not been previously associated with disease states, unlike the extensively characterised DN2 subset. Therefore, our study may help uncover more about this B cell population. This observation of the increased recent germinal centre emigrant DN1 B cells also fits with the report of increased frequency of T follicular helper cells in IgAN patients (Zhang et al., 2014).

We found a correlation between the $CD27^-$ precursors of IgA-expressing plasmablasts and serum LPS levels, that implicates mucosal immunity in the differentiation of these cells. LPS could directly contribute to class-switching in activated B cells as previously observed (Xu et al., 2008). In support of direct activation, tonsillar B cells from IgAN patients have been shown to produce increased IgA in response to LPS stimulation (Liu et al., 2011). Therefore, LPS may act at multiple stages of B cell activation to not only induce class-switching and IgA production, but to also regulate IgA glycosylation. An alternative explanation for the observed correlation between IgA^+CD27^- B cells and LPS could be that both are elevated because of intestinal inflammation, which may promote the generation of IgA^+CD27^- B cells and increase intestinal permeability. Supporting the mucosa as a site of origin for these IgA expressing B cells, IgAN patients have an increased frequency of IgA^+ B cells that express the mucosal homing marker CC chemokine receptor 9 (CCR9) (Sallustio et al., 2021a). Tonsillectomy, which has shown some therapeutic benefit in IgAN (Hirano et al., 2019), may potentially eliminate the site where these B cells are generated or where they migrate to (Wu et al., 2013). This may also help explain why B cell depletion therapies have shown inconsistent efficacy in IgAN, despite the central role of B cells in its pathogenesis – as mucosal niches may retain a significant proportion of precursor cells that are not effectively targeted by such treatments (Lafayette et al., 2017). Recent findings of disease-modifying effects of enteral budesonide in IgAN further implicate mucosal sites in driving immunopathogenesis (Smerud et al., 2011).

In our cohort of IgAN patients, the distribution of men, as well as the age and BMI, was found to be like that reported in other studies focusing on IgAN. Clinically, patients exhibited lower protein excretion, yet their eGFR was worse when compared to the results of other studies evaluating B cells in IgAN (Sallustio et al., 2021b; Wang et al., 2014). Of note, a limitation of the study is that our cohort consisted entirely of white Eastern Europeans and thus the B cell activation pathway remains to be investigated in non-European cohorts.

Now that we have identified the aberrant B cell differentiation pathways in IgAN, important further questions can be addressed. Key questions remain about the site of induction and long-term residence of IgA-expressing plasmablast precursors – are these cells generated and maintained in mucosal tissues, the bone marrow, or both, and is this pattern consistent among IgAN patients? Can specific targets be identified to selectively deplete or inhibit the differentiation of the pathogenic $IgA^{+}CD27^{-}$ B cells subset?! What antigens are IgA-expressing B cells in IgAN responding to – dietary or microbial components – and how diverse is the IgA response within an individual and across patients?

To explore whether microbial composition might influence the antigenic targets of IgA-expressing B cells in IgAN, we examined the gut microbiome profiles of affected individuals. It was a non-interventional study that did not establish causal relationships between findings. Our results aligned with previous gut microbiome studies in the Latvian population, which have identified *Prevotella* as the most common genus, showing a similar microbial community composition between the IgAN and HC groups. The high consumption of a plant-based, high-fibre diet is plausibly the primary reason for the high abundance of *Prevotella*. Interestingly, the data from our cohort in Latvia are like those of non-western populations (India, Peru, Tanzania, and Madagascar) (De Filippis et al., 2019). In contrast, the gut microbiome of Western populations, such as those in the United States and Spain, which consume a typical Westernised diet (rich in protein and fat and low in plant-based fibres), is enriched mainly in *Bacteroides* and *Ruminococcus*, with a very low abundance of *Prevotella* (Prasoodanan et al., 2021). According to a recent meta-analysis of gut microbiome characteristics in IgAN patients, which involved 11 cross-sectional studies and included 652 individuals, no consistent significant variations in the abundance of specific bacteria were noted across the different studies. For example, the *Bacteroides* genus had a greater relative abundance in patients with IgAN than in healthy individuals in three studies, a lower abundance in three studies, and no significant differences in four studies. Similarly, ambiguous data were found for *Streptococcus*, with higher abundances in patients with IgAN in two studies, lower abundances in one study, and no significant changes in eight studies (Han et al., 2022).

The differential abundance analysis in our study revealed that *Butyrococcus* and *Eubacterium rectale* (*Agathobacter rectalis*) were less abundant in IgAN patients than in healthy controls. Both bacteria produce butyrate from carbohydrates (Geirnaert et al., 2014). *E.rectale* preferentially colonises the mucus layer, thereby enhancing the bioavailability of butyrate for colon epithelial cells (El Aidy et al., 2013). Butyrate promotes intestinal barrier function by strengthening tight junctions and producing mucin and antimicrobial peptides and

is essential for the differentiation of CD4-positive regulatory T cells (Tregs), which suppress immune responses (Furusawa et al., 2013; Riviere et al., 2016). According to Yang et al, the number of Tregs is decreased in IgAN patients (Yang et al., 2015). Moreover, *Agathobacter rectalis* was the most prevalent bacteria in nonprogressors, patients with a favourable prognosis. These results highlight the potential importance of butyrate substitutions or dietary interventions. Butyrate-producing bacteria are predominantly slow-growing anaerobes, and their reduced abundance may be influenced by uremic toxins, gut mucosal inflammation, and the overgrowth of other bacterial species. In the intestinal microbiota of patients with IgAN, we observed an increased relative abundance of mucin-degrading bacteria, including *Akkermansia muciniphila*. This Gram-negative bacterium is an important modulator of the gut immune system, promoting the stimulation of cytokines such as IL-10 and enhancing secretory IgA production (Rodrigues et al., 2022). Another recent study found that IgA1 is deglycosylated by *Akkermansia muciniphila* both in vitro and within the intestinal lumen of mice, generating neo-epitopes that are recognised by autoreactive IgG in the sera of patients with IgAN. Following deglycosylation in the mouse gut, IgA1 underwent retrotranscytosis across the intestinal epithelium, entered the circulation, and was subsequently deposited in the glomeruli of the kidneys (Gleeson et al., 2024).

We found no significant difference in gut microbial diversity between IgAN patients and healthy individuals. These findings suggest that not the gut microbiome composition or microbial diversity plays a crucial role in IgAN pathogenesis but, hypothetically, changes in microbial community function.

Increased nucleoside (adenosine, guanosine, and inosine) biosynthesis pathways were found in IgAN patients. Extracellular adenosine is increased during intestinal inflammation. A key contributing factor to the development of intestinal inflammation is intestinal barrier dysfunction, which is associated with an altered microbiome composition, bacterial infiltration, impaired cell junctions, loss of the mucus layer and acidification. This contributes to the release of ATP from injured cells, which is converted to the alarm molecule adenosine (Stepanova & Aherne, 2024). Adenosine is a potent endogenous anti-inflammatory agent that regulates the function of inflammatory cells via interaction with specific receptors expressed on lymphocytes, inhibiting Th17 differentiation and stimulating Treg differentiation (Hasko & Cronstein, 2013). Inosine is formed from the breakdown of adenosine and has been shown to exert powerful anti-inflammatory effects related to the activation of adenosine receptors (Gomez & Sitkovsky, 2003).

Guanosine is a fundamental component of nucleotides and is essential for DNA and RNA synthesis (Balan et al., 2019). These processes are vital in rapidly dividing cells, such

as immune cells (e. g. lymphocytes and plasma cells), which require substantial amounts of nucleotides to support their proliferation during immune response. Lymphocytes and plasma cells are highly metabolically active during activation and expansion, as they produce antibodies and mediate immune responses. The increased demand for guanosine and other purine nucleotides in these cells aligns with their role in immune activation and inflammation, particularly in conditions such as IgAN, where aberrant immune responses are implicated. Another pathway, that is involved in the proliferative and inflammatory process – glycolysis from glucose 6-phosphate, was increased in IgAN patients compared with HC. Glycolysis is typically used as an energy source and is known to be upregulated in dividing cells (Ghazi et al., 2019).

The 4-hydroxyphenylacetate degradation pathway was more prominent in healthy controls than in IgAN patients. 4-Hydroxyphenylacetate is a common product during the fermentation of aromatic amino acids, particularly in the L-tyrosine degradation pathway, which is carried out by several *Escherichia coli* strains and generates pyruvate and succinate as end products (Kim et al., 2025). Higher succinate production by the gut microbiota is promoted by a high-protein diet (Tan et al., 2022). Usually, chronic kidney disease patients are recommended to decrease protein intake in their diet, resulting in potentially increased protein consumption in healthy individuals.

Another pathway that was decreased in IgAN patients – the sulfoquinovose degradation I pathway. Sulfoquinovose is a plant-derived sulfonated monosaccharide that serves as the polar headgroup of the sulfolipids in photosynthetic membranes. The final product of this pathway is glycerone phosphate, which powers the cell via glycolysis from glucose 6-phosphate, and 2,3-dihydroxypropane-1-sulfonate in most individuals fermented mainly by *E. rectale* (Hanson et al., 2021). Afterwards, it is excreted and can be further degraded by other bacteria and serves as a source of sulphite (Burrichter et al., 2018). As mentioned previously, *E. rectale* in our study was less abundant in IgAN patients, which confirms the possibility of delayed sulfoquinovose degradation. To date, there are no other studies in IgAN patients showing this pathway alteration.

Previous studies have analysed the bacterial composition in progressors and nonprogressors. Nonprogressor patients were defined as having a 50 % decrease in daily proteinuria and stable kidney function (eGFR) after six months compared with baseline (de Angelis et al., 2014); however, metabolic pathways were not studied between the two groups. In our study, the progression rate was evaluated according to a significant GFR slope of 5 ml/min/1.73 m^2/year at a mean follow-up time of 24 months, which is usually irreversible. Pathways enriched in progressors were connected to phospholipid synthesis in bacteria, which

are essential components of bacterial cell membranes. Gram-negative bacteria have a cell envelope composed of three distinct layers: the inner membrane, a periplasmic space containing the peptidoglycan cell wall, and the outer membrane, with its inner leaflet containing phospholipids and its outer leaflet predominantly composed of lipopolysaccharides (Morris & Mitchell, 2023). Phospholipid synthesis may be adapted to increase bacterial survival, colonisation, or competition.

The main limitation of the microbiome study part is its small sample size, which restricts confounder control and the detection of less prevalent microbial taxa. Additionally, while we employed a data-driven approach, using PERMANOVA to select covariates for differential abundance and pathway analyses, we acknowledge that this method does not account for potential unmeasured confounders. Factors not captured in our dataset, such as dietary patterns, medication use, or environmental exposures, could influence microbiome composition and function and thus may impact our findings. Given the strong evidence of IgAN-related shifts in gut microbiome functions, future studies may benefit from integrating metabolomics or metatranscriptomics data to provide deeper insights into the functional consequences of these microbial alterations. Additionally, investigating the effects of diet and probiotic supplementation on IgAN progression and immune cell dynamics remains an important avenue for future research.

The renoprotective effects of butyrate have been observed in various types of kidney diseases: in cisplatin-induced kidney injury (Favero et al., 2024), diabetic kidney disease (Zhou et al., 2022), obesity-related glomerulopathy (Shi et al., 2025), septic kidney injury modelled by lipopolysaccharide administration. In the latter model, sodium butyrate exerted nephroprotective effects by modulating TLR 2/4 signalling to regulate β-defensin 2 expression, thereby reducing inflammation (Dou et al., 2022). Another proposed mechanism involves the inhibition of both pyroptosis and apoptosis (Tian et al., 2025). As lipopolysaccharides derived from gut bacteria contribute to IgAN pathogenesis by promoting IgA1 overproduction and hypogalactosylation through TLR4 activation (Zhu et al., 2024), and given the decreased abundance of butyrate-producing bacteria observed in IgAN patients, future studies should investigate the potential therapeutic benefits of butyrate supplementation in IgAN management.

We have reported associations between specific microbial taxa in IgAN patients compared to healthy individuals, as well as in relation to kidney function decline. However, such associations do not imply causation. It remains essential to determine whether these microbiome alterations are a causal factor in IgAN development or a consequence of disease process. A combination of advanced computational approaches, animal models, and clinical

trials is essential to clarify the role of gut microbiome alterations in disease pathogenesis. These efforts should also account for the critical influence of diet on the gut–kidney axis.

Can the observed changes in the gut microbiome and B cells be the result of CKD? To minimise potential CKD-related effects, patients receiving kidney replacement therapy were excluded. With respect to B cells, CKD in general is associated with reduced memory B cells and impaired adaptive immunity. However, the specific pattern of increased naïve B cells and defective IgA memory differentiation leading to the formation of Gd-IgA1-secreting plasmablasts is more characteristic of IgAN. Some gut microbiome changes can indeed be associated with CKD; however, galactose-deficient IgA1 was the major factor accounting for a greater proportion of the observed variations in metabolic pathways, suggesting that these changes may be characteristic of patients with IgAN specifically. For future microbiome studies, detailed inclusion criteria should be applied to minimise possible confounding effects – for example, including only CKD patients with an eGFR > 60 ml/min.

Our IgAN research group plans to continue investigating the disease's pathogenesis by integrating analyses of B cell composition, with a particular focus on the interplay between the previously described $IgA^{+}CD27^{-}$ B cells and functional pathways of the gut microbiome. The next project will combine flow cytometry, single-cell transcriptional profiling, and confocal microscopy of mucosa-associated lymphoid tissue – specifically Peyer's patches – to identify the factors driving altered B cell activation in IgAN. We will employ cultures of sorted B cells and *in vitro* Peyer's patches models to explore what drives the differentiation of Gd-$IgA1^{+}$ B cells and antibody-secreting cells. Together, these approaches aim to fill a critical knowledge gap concerning the source and differentiation pathways of B cells involved in IgAN pathogenesis.

Conclusions

1 Patients with IgAN who have risk factors such as male gender, higher scores for tubular atrophy/interstitial fibrosis, and elevated diastolic blood pressure have an unfavourable prognosis for kidney survival over a five-year period, resulting in faster decline of renal function and progression to ESKD.

2 The observed and predicted risks using IIgANPT were similar, indicating that this tool can be effectively applied in the Latvian population.

3 Dysregulation of mucosal immunity drives the increased naïve B cell activation in germinal centres, giving rise to IgA+CD27-CD21+ B cells and subsequently IgA-producing plasmablasts.

4 Compared to healthy controls, patients with IgAN exhibit a reduction in butyrate-producing bacteria, which are essential for maintaining intestinal barrier function. Functional profiling of the gut microbiome in these patients suggests immune activation and inflammation, as indicated by increased activity in various nucleoside biosynthesis pathways.

Proposals

For better IgAN diagnostics in Latvia, urinalysis should be performed as a screening method at least once in adults aged 18–30 years and in all patients with hypertension. Patients with any grade of proteinuria or hematuria should be evaluated for kidney biopsy and receive follow up care from a general practitioner or nephrologist, depending on the clinical manifestations.

As IgAN is a heterogeneous disease with an unfavourable prognosis, risk assessment based on clinical factors and the IIgANPT results should be performed at diagnosis and every six months during follow-up. For patients at higher risk of progression, more aggressive lifestyle modifications, including dietary guidance, along with optimal blood pressure control and the use of maximally tolerated agents to inhibit angiotensin II activity, should be initiated.

List of publications, reports and patents on the topic of the Thesis

Publications

1. **Popova, A**., Racenis, K., Briviba, M., Saksis, R., Saulite, M., Slisere, B., Berga-Svitina, E., Oleinika, K., Saulite, A. J., Seilis, J., Kroica, J., Cernevskis, H., Petersons, A., Klovins, J., Lejnieks, A., & Kuzema, V. (2025). Reduced butyrate-producing bacteria and altered metabolic pathways in the gut microbiome of immunoglobulin A nephropathy patients. *Sci Rep*, 15(1), 28011. doi: 10.1038/s41598-025-13629-5

2. **Popova, A**., Slisere, B., Racenis, K., Kuzema, V., Karklins, R., Saulite, M., Seilis, J., Saulite, A. J., Vasilvolfa, A., Vaivode, K., Pjanova, D., Kroica, J., Cernevskis, H., Lejnieks, A., Petersons, A., Oleinika, K. (2025). IgA class-switched CD27−CD21+ B cells in IgA nephropathy. *Nephrology Dialysis Transplantation*, Volume 40, Issue 3, March 2025, 505–515. doi: 10.1093/ndt/gfae173

3. Saulīte, A. J., **Popova, A**., Erts, R.. Rācenis, K., Kučāne, L., Pētersons, A., Laurinavičius, A., Čerņevskis, H., Kuzema, V. (2021). Renal Survival and Validation of Novel International Immunoglobulin A Nephropathy Prediction Tool in Latvian Population. Preliminary Data. *Proceedings of the Latvian Academy of Sciences. Section B. Natural. Exact. and Applied Sciences*. 75(5). 379–386. doi: 10.2478/prolas-2021-0055.

4. Kučāne, L., **Popova, A**., Kuzema, V., Lejnieks, A., Pētersons, A. (2020). Epidemiological, Clinical and Morphological Characteristics of Immunoglobulin A Nephropathy in Latvia. *Proceedings of the Latvian Academy of Sciences. Section B. Natural. Exact. and Applied Sciences*. 74(4): 227–231. doi: 10.2478/prolas-2020-0036.

Oral Presentations at international congresses and published abstracts in *Nephrology Dialysis Transplantation*

1. **Popova, A**. Halturina, M., Rācenis, K., Saulīte, M., Seilis, J., Saulite, A. J., Petersons, A., Kroiča, J., Cernevskis, H., Oļeiņika, K., Šlisere, B., Lejnieks, A., Kuzema, V. (2023). Montreal Cognitive Assessment (MOCA) and Dysmorphic Red Blood Cells in Patients with Immunoglobulin a Nephropathy. *Nephrology Dialysis Transplantation*. vol. 38. no. Suppl.1. 5133. I338–I339. doi: 10.1093/ndt/gfad063c_5133

2. **Popova, A**., Rācenis, K., Kuzema, V., Saulīte, A. J., Saulīte, M., Broks, R., Oļeiņika, K., Šlisere, B., Petersons, A., Laurinavicius, A., Cernevkis, H., Lejnieks, A., Kroiča, J. (2022). Leucine-Rich Alpha-2-Glycoprotein as a Potential Marker of Mesangial Cell Proliferation in Immunoglobulin a Nephropathy. *Nephrology Dialysis Transplantation*. 37(Supplement_3). i293–i293. doi: 10.1093/ndt/gfac070.019

3. **Popova, A**., Rācenis, K., Saulite, A. J., Vasiļvolfa, A., Pētersons, A., Čerņevskis, H., Kuzema, V. (2021). Bedside Urine Sediment Examination in Immunoglobulin A Nephropathy Patients Performed by Nephrologists. *Nephrology Dialysis Transplantation*. Volume 36. Issue Supplement_1. doi: 10.1093/ndt/gfab104.0077

Oral Presentations at other international congresses and conferences

1. **Popova, A**. Are There Specific Changes in Microbial Composition in Patients with Immunoglobulin A Nephropathy? Rīga Stradiņš University International Research Conference on Medical and Health Care Sciences "Knowledge for Use in Practice". Abstracts. 26–28 March 2025. 122.

2. **Popova, A**. Gut Microbiome Characteristics in IgA nephropathy patients. XVII Baltic Nephrology Conference. 4 October 2024, Tartu, Estonia.

3. **Popova, A**., Rācenis, K., Saulīte, M., Seilis, J., Šlisere, B., Oļeinika, K., Saulīte, J. A., Kuzema, V., Kroiča, J., Lejnieks, A., Pētersons, A., Čerņevskis, H. (2023). The Role of Microbiome in Pathogenesis of Immunoglobulin A Nephropathy. Rīga Stradiņš University International Research Conference on Medical and Health Care Sciences "Knowledge for Use in Practice". Abstracts. 27–31 March 2023.

4. Halturina, M., **Popova, A**., Rācenis, K., Saulīte, M., Pētersons, A., Saulīte, A. J., Seilis, J., Čerņevskis, H., Kroiča, J., Lejnieks, A., Oļeiņika, K., Šlisere, B., Kuzema, V. (2022). Montreal Cognitive Assessment (MoCA) for Cognitive Screening in Patients with IgA Nephropathy compared with a control group. XVI Baltic Nephrology Conference. Abstracts. 6–8 October 2022. 49, Latvia.
5. **Popova, A**., Rācenis, K., Šlisere, B., Oleinika, K., Vasiļvolfa, A., Saulīte, A. J., Kuzema, V., Kroiča, J., Lejnieks, A., Berga-Švītiņa, E., Pētersons, A., Čerņevskis, H. (2021). Dissecting the interplay between intestinal dysbiosis and B cell function in the pathogenesis of immunoglobulin A nephropathy. Rīga Stradiņš University International Research Conference on Medical and Health Care Sciences "Knowledge for Use in Practice". Abstracts. 22–26 March 2021. 434.
6. **Popova, A**. IgA nephropathy research in Latvia – national project. XV Baltic Nephrology Conference "UpToDate in Nephrology, Dialysis and Kidney Transplantation". 12 December 2020, Lithuania.

Theses at international congresses and conferences

1. Saulīte, M., Matusevica, L., **Popova, A**., Kuzema, V., Oļeiņika, K., Šlisere, B., Pētersons, A., Kroiča, J., Lejnieks, A., Rācenis, K. 2025. Risk Factors for IgA Nephropathy Progression: Insights beyond Galactose-Deficient IgA1 Levels. Rīga Stradiņš University International Research Conference on Medical and Health Care Sciences "Knowledge for Use in Practice". Abstracts. 26–28 March 2025. 123.
2. Saulīte, M., Matuseviča, L., **Popova, A**., Kuzema, V., Oļeiņika, K., Šlisere, B., Pētersons, A., Kroiča, J., Rācenis, K. 2024. The Ambiguous Role of Serum Gd-IgA1 in IgA Nephropathy: An Evaluation of Its Biomarker Potential. XVII Baltic Nephrology Conference. 4 October 2024, Tartu, Estonia.
3. Rācenis, K., Saulīte, A. J., **Popova, A**., Saulīte, M., Kroiča, J., Petersons, A., Cernevskis, H., Lejnieks, A., Oļeiņika, K., Šlisere, B., Seilis, J., Kuzema, V. (2022). Sars-COV-2 Vaccination DID Not Affect the Clinical Course of IgA Nephropathy in Latvian Adult Cohort. *Nephrology Dialysis Transplantation*. 37(Supplement_3). i145–i146. doi: 10.1093/ndt/gfac067.012
4. Halturina, M., **Popova, A**. (2022). Montreal Cognitive Assessment (MoCA) for Cognitive Screening in Patients with IgA Nephropathy. 17th Warsaw International Medical Congress. 06–08 May 2022. 100.
5. **Popova, A**., Saulīte, A. J., Rācenis, K., Vasiļvolfa, A., Kroiča, J., Pētersons, A., Lejnieks, A., Oleinika, K., Čerņevskis, H., Kuzema, V. (2021). Serum complement C3 and C4 levels: prognostic factors in immunoglobulin A nephropathy. Rīga Stradiņš University International Research Conference on Medical and Health Care Sciences "Knowledge for Use in Practice". Abstracts. 22–26 March 2021. 524.
6. Šlisere, B., **Popova, A**., Rācenis, K., Vasiļvolfa, A., Berga-Švītiņa, E., Imša, K., Saulīte, A. J., Kuzema, V., Laurinavicius, A., Lejnieks, A., Kroiča, J., Pētersons, A., Čerņevskis, H., Oleinika, K. (2021). Altered B-cell populations in IgA nephropathy. Rīga Stradiņš University International Research Conference on Medical and Health Care Sciences "Knowledge for Use in Practice". Abstracts. 22–26 March 2021. 565.
7. Bernšteine, A. J., **Popova, A**., Kučāne, L., Rācenis, K., Kuzema, V., Pētersons, A. (2020). Immunoglobulin A nephropathy prediction tool validation in Latvian population. XV Baltic Nephrology Conference UpToDate in Nephrology. Dialysis and Kidney Transplantation. Abstracts. 8. Lithuania.
8. Šlisere, B., **Popova, A**., Rācenis, K., Vasiļvolfa, A., Berga-Švītiņa, E., Kuzema, V., Lejnieks, A., Kroiča, J., Pētersons, A., Čerņevskis, H., Oļeiņika, K. (2020). Characterization of peripheral B-cells in IgA nephropathy. XV Baltic Congress in Laboratory Medicine. Riga. Latvia.
9. Saulīte, A. J., **Popova, A**., Kučāne, L., Kuzema, V., Pētersons, A. (2020). Kidney survival analysis in immunoglobulin A nephropathy patients. International Scientific Conference of the University of Latvia. 12 March 2020. 171.
10. Babičeva, P., **Popova, A**. (2021). Assessment of dietary habits in patients with immunoglobulin A nephropathy. Warsaw International Medical Congress. 29–30 May 2021. 68

References

1. Bagchi, S., Upadhyay, A. D., Barwad, A., Singh, G., Subbiah, A., Yadav, R. K., Mahajan, S., Bhowmik, D., & Agarwal, S. K. (2022). The International IgA Nephropathy Network Prediction Tool Underestimates Disease Progression in Indian Patients. *Kidney Int Rep*, *7*(6), 1210–1218. https://doi.org/10.1016/j.ekir.2022.03.016

2. Balan, M., Chakraborty, S., & Pal, S. (2019). Signaling Molecules in Posttransplantation Cancer. *Clin Lab Med*, *39*(1), 171–183. https://doi.org/10.1016/j.cll.2018.10.006

3. Barbour, S. J., Coppo, R., Zhang, H., Liu, Z. H., Suzuki, Y., Matsuzaki, K., Katafuchi, R., Er, L., Espino-Hernandez, G., Kim, S. J., Reich, H. N., Feehally, J., Cattran, D. C., & International Ig, A. N. N. (2019). Evaluating a New International Risk-Prediction Tool in IgA Nephropathy. *JAMA Intern Med*, *179*(7), 942–952. https://doi.org/10.1001/jamainternmed.2019.0600

4. Bon, G., Jullien, P., Masson, I., Sauron, C., Dinic, M., Claisse, G., Pelaez, A., Thibaudin, D., Mohey, H., Alamartine, E., Mariat, C., & Maillard, N. (2023). Validation of the international IgA nephropathy prediction tool in a French cohort beyond 10 years after diagnosis. *Nephrol Dial Transplant*, *38*(10), 2257–2265. https://doi.org/10.1093/ndt/gfad048

5. Bugatti, S., Vitolo, B., Caporali, R., Montecucco, C., & Manzo, A. (2014). B cells in rheumatoid arthritis: from pathogenic players to disease biomarkers. *Biomed Res Int*, *2014*, 681678. https://doi.org/10.1155/2014/681678

6. Burrichter, A., Denger, K., Franchini, P., Huhn, T., Muller, N., Spiteller, D., & Schleheck, D. (2018). Anaerobic Degradation of the Plant Sugar Sulfoquinovose Concomitant With H(2)S Production: Escherichia coli K-12 and Desulfovibrio sp. Strain DF1 as Co-culture Model. *Front Microbiol*, *9*, 2792. https://doi.org/10.3389/fmicb.2018.02792

7. Cerutti, A. (2008). The regulation of IgA class switching. *Nat Rev Immunol*, *8*(6), 421–434. https://doi.org/10.1038/nri2322

8. Coppo, R., D'Arrigo, G., Tripepi, G., Russo, M. L., Roberts, I. S. D., Bellur, S., Cattran, D., Cook, T. H., Feehally, J., Tesar, V., Maixnerova, D., Peruzzi, L., Amore, A., Lundberg, S., Di Palma, A. M., Gesualdo, L., Emma, F., Rollino, C., Praga, M., . . . Group, E.-E. I. W. (2020). Is there long-term value of pathology scoring in immunoglobulin A nephropathy? A validation study of the Oxford Classification for IgA Nephropathy (VALIGA) update. *Nephrol Dial Transplant*, *35*(6), 1002–1009. https://doi.org/10.1093/ndt/gfy302

9. Coppo, R., Troyanov, S., Bellur, S., Cattran, D., Cook, H. T., Feehally, J., Roberts, I. S., Morando, L., Camilla, R., Tesar, V., Lunberg, S., Gesualdo, L., Emma, F., Rollino, C., Amore, A., Praga, M., Feriozzi, S., Segoloni, G., Pani, A., . . . Group, V. s. o. t. E.-E. I. W. (2014). Validation of the Oxford classification of IgA nephropathy in cohorts with different presentations and treatments. *Kidney Int*, *86*(4), 828–836. https://doi.org/10.1038/ki.2014.63

10. De Angelis, M., Montemurno, E., Piccolo, M., Vannini, L., Lauriero, G., Maranzano, V., Gozzi, G., Serrazanetti, D., Dalfino, G., Gobbetti, M., & Gesualdo, L. (2014). Microbiota and metabolome associated with immunoglobulin A nephropathy (IgAN). *PLoS One*, *9*(6), e99006. https://doi.org/10.1371/journal.pone.0099006

11. De Filippis, F., Pasolli, E., Tett, A., Tarallo, S., Naccarati, A., de Angelis, M., Neviani, E., Cocolin, L., Gobbetti, M., Segata, N., & Ercolini, D. (2019). Distinct Genetic and Functional Traits of Human Intestinal Prevotella copri Strains Are Associated with Different Habitual Diets. *Cell Host Microbe*, *25*(3), 444–453 e443. https://doi.org/10.1016/j.chom.2019.01.004

12. Deng, W., Tan, X., Zhou, Q., Ai, Z., Liu, W., Chen, W., Yu, X., & Yang, Q. (2018). Gender-related differences in clinicopathological characteristics and renal outcomes of Chinese patients with IgA nephropathy. *BMC Nephrol*, *19*(1), 31. https://doi.org/10.1186/s12882-018-0829-1

13. Dou, X., Yan, D., Ma, Z., Gao, N., & Shan, A. (2022). Sodium butyrate alleviates LPS-induced kidney injury via inhibiting TLR2/4 to regulate rBD2 expression. *J Food Biochem*, *46*(7), e14126. https://doi.org/10.1111/jfbc.14126

14. El Aidy, S., Van den Abbeele, P., Van de Wiele, T., Louis, P., & Kleerebezem, M. (2013). Intestinal colonization: how key microbial players become established in this dynamic process: microbial metabolic activities and the interplay between the host and microbes. *Bioessays*, *35*(10), 913–923. https://doi.org/10.1002/bies.201300073

15. Favero, C., Pintor-Chocano, A., Sanz, A., Ortiz, A., & Sanchez-Nino, M. D. (2024). Butyrate promotes kidney resilience through a coordinated kidney protective response in tubular cells. *Biochem Pharmacol*, *224*, 116203. https://doi.org/10.1016/j.bcp.2024.116203

16. Furusawa, Y., Obata, Y., Fukuda, S., Endo, T. A., Nakato, G., Takahashi, D., Nakanishi, Y., Uetake, C., Kato, K., Kato, T., Takahashi, M., Fukuda, N. N., Murakami, S., Miyauchi, E., Hino, S., Atarashi, K., Onawa, S., Fujimura, Y., Lockett, T., . . . Ohno, H. (2013). Commensal microbe-derived butyrate induces the differentiation of colonic regulatory T cells. *Nature*, *504*(7480), 446–450. https://doi.org/10.1038/nature12721

17. Geddes, C. C., Rauta, V., Gronhagen-Riska, C., Bartosik, L. P., Jardine, A. G., Ibels, L. S., Pei, Y., & Cattran, D. C. (2003). A tricontinental view of IgA nephropathy. *Nephrol Dial Transplant*, *18*(8), 1541–1548. https://doi.org/10.1093/ndt/gfg207

18. Geirnaert, A., Steyaert, A., Eeckhaut, V., Debruyne, B., Arends, J. B., Van Immerseel, F., Boon, N., & Van de Wiele, T. (2014). Butyricicoccus pullicaecorum, a butyrate producer with probiotic potential, is intrinsically tolerant to stomach and small intestine conditions. *Anaerobe*, *30*, 70–74. https://doi.org/10.1016/j.anaerobe.2014.08.010

19. Ghazi, S., Polesel, M., & Hall, A. M. (2019). Targeting glycolysis in proliferative kidney diseases. *Am J Physiol Renal Physiol*, *317*(6), F1531–F1535. https://doi.org/10.1152/ajprenal.00460.2019

20. Gleeson, P. J., Benech, N., Chemouny, J., Metallinou, E., Berthelot, L., da Silva, J., Bex-Coudrat, J., Boedec, E., Canesi, F., Bounaix, C., Morelle, W., Moya-Nilges, M., Kenny, J., O'Mahony, L., Saveanu, L., Arnulf, B., Sannier, A., Daugas, E., Vrtovsnik, F., . . . Monteiro, R. C. (2024). The gut microbiota posttranslationally modifies IgA1 in autoimmune glomerulonephritis. *Sci Transl Med*, *16*(740), eadl6149. https://doi.org/10.1126/scitranslmed.adl6149

21. Gomez, G., & Sitkovsky, M. V. (2003). Differential requirement for A2a and A3 adenosine receptors for the protective effect of inosine in vivo. *Blood*, *102*(13), 4472–4478. https://doi.org/10.1182/blood-2002-11-3624

22. Haaskjold, Y. L., Lura, N. G., Bjorneklett, R., Bostad, L., Bostad, L. S., & Knoop, T. (2023). Validation of two IgA nephropathy risk-prediction tools using a cohort with a long follow-up. *Nephrol Dial Transplant*, *38*(5), 1183–1191. https://doi.org/10.1093/ndt/gfac225

23. Han, S., Shang, L., Lu, Y., & Wang, Y. (2022). Gut Microbiome Characteristics in IgA Nephropathy: Qualitative and Quantitative Analysis from Observational Studies. *Front Cell Infect Microbiol*, *12*, 904401. https://doi.org/10.3389/fcimb.2022.904401

24. Hanson, B. T., Dimitri Kits, K., Loffler, J., Burrichter, A. G., Fiedler, A., Denger, K., Frommeyer, B., Herbold, C. W., Rattei, T., Karcher, N., Segata, N., Schleheck, D., & Loy, A. (2021). Sulfoquinovose is a select nutrient of prominent bacteria and a source of hydrogen sulfide in the human gut. *ISME J*, *15*(9), 2779–2791. https://doi.org/10.1038/s41396-021-00968-0

25. Hasko, G., & Cronstein, B. (2013). Regulation of inflammation by adenosine. *Front Immunol*, *4*, 85. https://doi.org/10.3389/fimmu.2013.00085

26. Hirano, K., Matsuzaki, K., Yasuda, T., Nishikawa, M., Yasuda, Y., Koike, K., Maruyama, S., Yokoo, T., Matsuo, S., Kawamura, T., & Suzuki, Y. (2019). Association Between Tonsillectomy and Outcomes in Patients With Immunoglobulin A Nephropathy. *JAMA Netw Open*, *2*(5), e194772. https://doi.org/10.1001/jamanetworkopen.2019.4772

27. Kidney Disease: Improving Global Outcomes Glomerular Diseases Work, G. (2021). KDIGO 2021 Clinical Practice Guideline for the Management of Glomerular Diseases. *Kidney Int*, *100*(4S), S1–S276. https://doi.org/10.1016/j.kint.2021.05.021

28. Kim, S., Chen, J., Cheng, T., Gindulyte, A., He, J., He, S., Li, Q., Shoemaker, B. A., Thiessen, P. A., Yu, B., Zaslavsky, L., Zhang, J., & Bolton, E. E. (2025). PubChem 2025 update. *Nucleic Acids Res*, *53*(D1), D1516-D1525. https://doi.org/10.1093/nar/gkae1059

29. Kiryluk, K., Novak, J., & Gharavi, A. G. (2013). Pathogenesis of immunoglobulin A nephropathy: recent insight from genetic studies. *Annu Rev Med*, *64*, 339–356. https://doi.org/10.1146/annurev-med-041811-142014

30. Lafayette, R. A., Canetta, P. A., Rovin, B. H., Appel, G. B., Novak, J., Nath, K. A., Sethi, S., Tumlin, J. A., Mehta, K., Hogan, M., Erickson, S., Julian, B. A., Leung, N., Enders, F. T., Brown, R., Knoppova, B., Hall, S., & Fervenza, F. C. (2017). A Randomized, Controlled Trial of Rituximab in IgA Nephropathy with Proteinuria and Renal Dysfunction. *J Am Soc Nephrol*, *28*(4), 1306–1313. https://doi.org/10.1681/ASN.2016060640

31. Launay, P., Grossetete, B., Arcos-Fajardo, M., Gaudin, E., Torres, S. P., Beaudoin, L., Patey-Mariaud de Serre, N., Lehuen, A., & Monteiro, R. C. (2000). Fcalpha receptor (CD89) mediates the development of immunoglobulin A (IgA) nephropathy (Berger's disease). Evidence for pathogenic soluble receptor-Iga complexes in patients and CD89 transgenic mice. *J Exp Med*, *191*(11), 1999–2009. https://doi.org/10.1084/jem.191.11.1999

32. Liu, H., Peng, Y., Liu, F., Xiao, W., Zhang, Y., & Li, W. (2011). Expression of IgA class switching gene in tonsillar mononuclear cells in patients with IgA nephropathy. *Inflamm Res*, *60*(9), 869–878. https://doi.org/10.1007/s00011-011-0347-0

33. Mohr, A. E., Crawford, M., Jasbi, P., Fessler, S., & Sweazea, K. L. (2022). Lipopolysaccharide and the gut microbiota: considering structural variation. *FEBS Lett*, *596*(7), 849–875. https://doi.org/10.1002/1873-3468.14328

34. Moriyama, T., Tanaka, K., Iwasaki, C., Oshima, Y., Ochi, A., Kataoka, H., Itabashi, M., Takei, T., Uchida, K., & Nitta, K. (2014). Prognosis in IgA nephropathy: 30-year analysis of 1,012 patients at a single center in Japan. *PLoS One*, *9*(3), e91756. https://doi.org/10.1371/journal.pone.0091756

35. Morris, K. N., & Mitchell, A. M. (2023). Phosphatidylglycerol Is the Lipid Donor for Synthesis of Phospholipid-Linked Enterobacterial Common Antigen. *J Bacteriol*, *205*(1), e0040322. https://doi.org/10.1128/jb.00403-22

36. Nagy, J., Kovacs, T., & Wittmann, I. (2005). Renal protection in IgA nephropathy requires strict blood pressure control. *Nephrol Dial Transplant*, *20*(8), 1533–1539. https://doi.org/10.1093/ndt/gfh920

37. Papasotiriou, M., Stangou, M., Chlorogiannis, D., Marinaki, S., Xydakis, D., Sampani, E., Lioulios, G., Kapsia, E., Zerbala, S., Koukoulaki, M., Moustakas, G., Fokas, S., Dounousi, E., Duni, A., Papadaki, A., Damianakis, N., Bacharaki, D., Stylianou, K., Gakiopoulou, H., . . . Goumenos, D. S. (2022). Validation of the International IgA Nephropathy Prediction Tool in the Greek Registry of IgA Nephropathy. *Front Med (Lausanne)*, *9*, 778464. https://doi.org/10.3389/fmed.2022.778464

38. Prasoodanan, P. K. V., Sharma, A. K., Mahajan, S., Dhakan, D. B., Maji, A., Scaria, J., & Sharma, V. K. (2021). Western and non-western gut microbiomes reveal new roles of Prevotella in carbohydrate metabolism and mouth-gut axis. *NPJ Biofilms Microbiomes*, *7*(1), 77. https://doi.org/10.1038/s41522-021-00248-x

39. Riviere, A., Selak, M., Lantin, D., Leroy, F., & De Vuyst, L. (2016). Bifidobacteria and Butyrate-Producing Colon Bacteria: Importance and Strategies for Their Stimulation in the Human Gut. *Front Microbiol*, *7*, 979. https://doi.org/10.3389/fmicb.2016.00979

40. Rodrigues, V. F., Elias-Oliveira, J., Pereira, I. S., Pereira, J. A., Barbosa, S. C., Machado, M. S. G., & Carlos, D. (2022). Akkermansia muciniphila and Gut Immune System: A Good Friendship That Attenuates Inflammatory Bowel Disease, Obesity, and Diabetes. *Front Immunol*, *13*, 934695. https://doi.org/10.3389/fimmu.2022.934695

41. Sallustio, F., Curci, C., Chaoul, N., Fonto, G., Lauriero, G., Picerno, A., Divella, C., Di Leo, V., de Angelis, M., Ben Mkaddem, S., Macchia, L., Gallone, A., Monteiro, R. C., Pesce, F., & Gesualdo, L. (2021a). High levels of gut-homing immunoglobulin A+ B lymphocytes support the pathogenic role of intestinal mucosal hyperresponsiveness in immunoglobulin A nephropathy patients. *Nephrol Dial Transplant*, *36*(9), 1765. https://doi.org/10.1093/ndt/gfaa344

42. Sallustio, F., Curci, C., Chaoul, N., Fonto, G., Lauriero, G., Picerno, A., Divella, C., Di Leo, V., de Angelis, M., Ben Mkaddem, S., Macchia, L., Gallone, A., Monteiro, R. C., Pesce, F., & Gesualdo, L. (2021b). High levels of gut-homing immunoglobulin A+ B lymphocytes support the pathogenic role of intestinal mucosal hyperresponsiveness in immunoglobulin A nephropathy patients. *Nephrol Dial Transplant*, *36*(3), 452–464. https://doi.org/10.1093/ndt/gfaa264

43. Sato, S., Fujimoto, M., Hasegawa, M., & Takehara, K. (2004). Altered blood B lymphocyte homeostasis in systemic sclerosis: expanded naive B cells and diminished but activated memory B cells. *Arthritis Rheum*, *50*(6), 1918–1927. https://doi.org/10.1002/art.20274

44. Schimpf, J. I., Klein, T., Fitzner, C., Eitner, F., Porubsky, S., Hilgers, R. D., Floege, J., Groene, H. J., & Rauen, T. (2018). Renal outcomes of STOP-IgAN trial patients in relation to baseline histology (MEST-C scores). *BMC Nephrol*, *19*(1), 328. https://doi.org/10.1186/s12882-018-1128-6

45. Scionti, K., Molyneux, K., Selvaskandan, H., Barratt, J., & Cheung, C. K. (2022). New Insights into the Pathogenesis and Treatment Strategies in IgA Nephropathy. *Glomerular Dis*, *2*(1), 15–29. https://doi.org/10.1159/000519973

46. Shi, Y., Xing, L., Zheng, R., Luo, X., Yue, F., Xiang, X., Qiu, A., Xie, J., Russell, R., & Zhang, D. (2025). Butyrate attenuates high-fat diet-induced glomerulopathy through GPR43-Sirt3 pathway. *Br J Nutr*, *133*(1), 1–10. https://doi.org/10.1017/S0007114524002964

47. Smerud, H. K., Barany, P., Lindstrom, K., Fernstrom, A., Sandell, A., Pahlsson, P., & Fellstrom, B. (2011). New treatment for IgA nephropathy: enteric budesonide targeted to the ileocecal region ameliorates proteinuria. *Nephrol Dial Transplant*, *26*(10), 3237–3242. https://doi.org/10.1093/ndt/gfr052

48. Stepanova, M., & Aherne, C. M. (2024). Adenosine in Intestinal Epithelial Barrier Function. *Cells*, *13*(5). https://doi.org/10.3390/cells13050381

49. Tan, J., Ni, D., Taitz, J., Pinget, G. V., Read, M., Senior, A., Wali, J. A., Elnour, R., Shanahan, E., Wu, H., Chadban, S. J., Nanan, R., King, N. J. C., Grau, G. E., Simpson, S. J., & Macia, L. (2022). Dietary protein increases T-cell-independent sIgA production through changes in gut microbiota-derived extracellular vesicles. *Nat Commun*, *13*(1), 4336. https://doi.org/10.1038/s41467-022-31761-y

50. Tian, X., Yuan, L., & Zeng, Y. (2025). Butyrate attenuates SA-AKI by inhibiting pyroptosis via the STING-GSDMD axis. *Biochem Biophys Res Commun*, *743*, 151143. https://doi.org/10.1016/j.bbrc.2024.151143

51. Wang, Y. Y., Zhang, L., Zhao, P. W., Ma, L., Li, C., Zou, H. B., & Jiang, Y. F. (2014). Functional implications of regulatory B cells in human IgA nephropathy. *Scand J Immunol*, *79*(1), 51–60. https://doi.org/10.1111/sji.12128

52. Wu, G., Peng, Y. M., Liu, F. Y., Xu, D., & Liu, C. (2013). The role of memory B cell in tonsil and peripheral blood in the clinical progression of IgA nephropathy. *Hum Immunol*, *74*(6), 708–712. https://doi.org/10.1016/j.humimm.2012.10.028

53. Xu, H., Liew, L. N., Kuo, I. C., Huang, C. H., Goh, D. L., & Chua, K. Y. (2008). The modulatory effects of lipopolysaccharide-stimulated B cells on differential T-cell polarization. *Immunology*, *125*(2), 218–228. https://doi.org/10.1111/j.1365-2567.2008.02832.x

54. Xu, L. L., Zhou, X. J., & Zhang, H. (2023). An Update on the Genetics of IgA Nephropathy. *J Clin Med*, *13*(1). https://doi.org/10.3390/jcm13010123

55. Yang, S., Chen, B., Shi, J., Chen, F., Zhang, J., & Sun, Z. (2015). Analysis of regulatory T cell subsets in the peripheral blood of immunoglobulin A nephropathy (IgAN) patients. *Genet Mol Res*, *14*(4), 14088–14092. https://doi.org/10.4238/2015.October.29.28

56. Zhang, L., Wang, Y., Shi, X., Zou, H., & Jiang, Y. (2014). A higher frequency of CD4(+)CXCR5(+) T follicular helper cells in patients with newly diagnosed IgA nephropathy. *Immunol Lett*, *158*(1-2), 101–108. https://doi.org/10.1016/j.imlet.2013.12.004

57. Zhang, Y., Guo, L., Wang, Z., Wang, J., Er, L., Barbour, S. J., Trimarchi, H., Lv, J., & Zhang, H. (2020). External Validation of International Risk-Prediction Models of IgA Nephropathy in an Asian-Caucasian Cohort. *Kidney Int Rep*, *5*(10), 1753–1763. https://doi.org/10.1016/j.ekir.2020.07.036

58. Zheng, Y., Wang, Y., Liu, S., Wu, J., Duan, S., Zhu, H., Wu, D., Cai, G., & Chen, X. (2018). Potential Blood Pressure Goals in IgA Nephropathy: Prevalence, Awareness, and Treatment Rates in Chronic Kidney Disease Among Patients with Hypertension in China (PATRIOTIC) Study. *Kidney Blood Press Res*, *43*(6), 1786–1795. https://doi.org/10.1159/000495636

59. Zhou, T., Xu, H., Cheng, X., He, Y., Ren, Q., Li, D., Xie, Y., Gao, C., Zhang, Y., Sun, X., Xu, Y., & Huang, W. (2022). Sodium Butyrate Attenuates Diabetic Kidney Disease Partially via Histone Butyrylation Modification. *Mediators Inflamm*, *2022*, 7643322. https://doi.org/10.1155/2022/7643322

60. Zhu, Y., He, H., Sun, W., Wu, J., Xiao, Y., Peng, Y., Hu, P., Jin, M., Liu, P., Zhang, D., Xie, T., Huang, L., He, W., Wei, M., Wang, L., Xu, X., & Tang, Y. (2024). IgA nephropathy: gut microbiome regulates the production of hypoglycosilated IgA1 via the TLR4 signaling pathway. *Nephrol Dial Transplant*, *39*(10), 1624–1641. https://doi.org/10.1093/ndt/gfae052

Acknowledgements

I express my deep gratitude to my scientific supervisors: *MD, PhD* Associate Professor **Viktorija Kuzema** for invaluable guidance, time and substantial assistance during the research and writing phases, unwavering faith in me, support, that allowed me to seamlessly integrate research work with clinical responsibilities in the department; and *Dr. med.* Professor **Juta Kroiča** for immeasurable knowledge and invaluable guidance provided consistently throughout the doctoral studies and thesis writing process.

Part of this research was conducted within the framework of a successfully approved No lzp-2019/1-0139 "Dissecting the interplay between intestinal dysbiosis and B cell function in the pathogenesis of immunoglobulin A nephropathy". I am very thankful to my colleagues from IgAN project group, particularly, *MD, PhD* Assistant Professor **Kārlis Rācenis**, Assistant Professor **Kristīne Oļeiņika**, with whom the concept of the project was conceived and executed, as well as **Anna Jana Saulīte** for her assistance with data management. Kārlis accompanied me during challenging moments of laboratory work and drawing on personal experience, served as a scientific consultant. Thanks to colleagues at Latvian Biomedical Research and Study Centre for their cooperation.

I would like to extend my sincere gratitude to *MD, PhD* Professor **Aivars Pētersons** – head of the Nephrology Centre for providing the opportunity to engage in scientific exploration and work in the field of Nephrology.